Exendin-based targeting of beta cells for in vivo monitoring of transplanted islets

Wael Arabi Eter

The research described in this thesis was performed at the Department of Radiology and Nuclear Medicine and was supported by the People Program (Marie Curie Actions) of the European Union's Seventh Framework Program FP7/2007-2013/ Under REA grant agreement number 289932

Printing of this thesis was financially supported by Radboud University Nijmegen

Design/lay-out
Promotie In Zicht, Arnhem

Print
Ipskamp Printing, Enschede

Exendin-based targeting of beta cells for in vivo monitoring of transplanted islets

Proefschrift

ter verkrijging van de graad van doctor
aan de Radboud Universiteit Nijmegen
op gezag van de rector magnificus prof. dr. J.H.J.M. van Krieken,
volgens besluit van het college van decanen
in het openbaar te verdedigen op 1 februari 2018
om 14.30 uur precies

door

Wael Arabi Eter
geboren op 10 juli 1988
te Hallsberg, Zweden

Promotoren
Prof. dr. Martin Gotthardt
Prof. dr. Ulf Ahlgren *(Umeå Universitet, Zweden)*

Copromotoren
Dr. Maarten Brom
Dr. Mijke Buitinga

Manuscriptcommissie
Prof. dr. Mihai G. Netea
Prof. dr. Peter H.A. Friedl
Prof. dr. Eckhart Lammert *(Heinrich-Heine-Universität Düsseldorf, Duitsland)*

Exendin-based targeting of beta cells for in vivo monitoring of transplanted islets

Doctoral Thesis

to obtain the degree of doctor
from Radboud University Nijmegen
on the authority of the Rector Magnificus prof. dr. J.H.J.M. van Krieken,
according to the decision of the Council of Deans
to be defended in public on Thursday, February 1, 2018
at 14.30 hours

by

Wael Arabi Eter
Born on 10 July, 1988
in Hallsberg (Sweden)

Supervisors
Prof. dr. Martin Gotthardt
Prof. dr. Ulf Ahlgren *(Umeå Universitet, Sweden)*

Co-supervisors
Dr. Maarten Brom
Dr. Mijke Buitinga

Doctoral Thesis Committee
Prof. dr. Mihai G. Netea
Prof. dr. Peter H.A. Friedl
Prof. dr. Eckhart Lammert *(Heinrich-Heine-Universität Düsseldorf, Germany)*

Table of Contents

List of Abbreviations

BCF	Beta-cell function
BCM	Beta-cell mass
Bq	Becquerels
GLP-1	Glucagon-like peptide 1
GLP-1R	Glucagon-like peptide 1 receptor
MRI	Magnetic Resonance Imaging
OPT	Optical Projection Tomography
PET	Positron Emission Tomography
SPECT	Single Photon Emission Computed Tomography
T1D	Type 1 diabetes
T2D	Type 2 diabetes
VEGFR-2	Vascular endothelial growth factor receptor 2

1

Outline of the thesis

Outline of the thesis

Diabetes mellitus is a group of metabolic diseases characterized by persistent hyperglycemia. The prevalence of diabetes is 415 million worldwide and the numbers are on the rise [1]. The underlying mechanisms of diabetes are auto-immune destruction of the insulin producing cells (β-cells), which is characteristic for type 1 diabetes, or insufficient insulin secretion due to insulin resistance, which is – together with other factors – typical for type 2 diabetes.

The most common approach to maintain blood glucose level within the physiological range (90-110 mg/dl, or 4-6 mmol/L) in T1D patients is to receive insulin injections on a daily basis. This approach is however associated with several disadvantages, such as regular episodes of hypoglycemia, potentially overall poor blood glucose control with the risk of developing long-term diabetes complications (such as blindness, cardiovascular disease, kidney failure etc.); alternative methods are therefore required.

Since the establishment of the Edmonton protocol by Chapiro et al. [2], pancreatic islet transplantation has become a promising experimental option for treating type 1 diabetes patients, where transplanted islets compensate for the β-cell loss in the pancreas, significantly reducing the necessity for insulin injections and reducing the rate of hypoglycemic episodes [3]. However, most subjects are reverted to using insulin 5 years after transplantation [4]. The leading causes of relapse are the poor rate of islet engraftment, hypoxia, gluco/lipotoxicity, auto-immunity and immunosuppression toxicity, all resulting in decline in islet survival and function [5, 6].

Intensive research was conducted during the past decades for improving the clinical outcome of islet transplantation, not only by elucidating the pathways that lead to β-cell loss and dysfunction, but also by understanding how the decrease in β-cell number, or β-cell mass (BCM), is linked to progressive relapse into hyperglycemia. Indeed, the relationship between BCM and their ability in maintaining normoglycemia (or function) is unclear, and the players that cause the discrepancy between BCM and function are multifactorial [7, 8].

To date, it remains difficult to quantify islet survival given that clinical functional tests cannot discriminate between BCM and function (BCF). A reliable non-invasive method is therefore needed to monitor graft survival, independently of its function. Such method should provide information regarding the number of surviving islets, and the technique should be applied repeatedly and non-invasively with regard to clinical implementation.

Radioactive-based imaging modalities (SPECT: Single Photon Emission Computed Tomography; PET: Positron Emission Tomography) are attractive technologies for non-invasive imaging of the β-cells after injection of β-cell specific radiotracers [9-11]. These techniques offer high sensitivity, prompting the detection of very small

differences in BCM. One promising tracer for β-cell imaging is radiolabeled exendin, which specifically accumulates in the β-cells after binding to the GLP-1R expressed on their surface. The utility of this radiotracer for imaging of islet transplants was demonstrated in a mouse model for islet transplantation where β-cells were visualized by PET after injection of Cu-64 or F-18 labeled exendin-4 and in a clinical case study where β-cells were visualized by SPECT after injection of ^{111}In-labeled exendin-4 [12, 13].

The main focus of this thesis is to determine the possibility to quantify BCM of islets transplanted in the skeletal muscle by SPECT in healthy (control model) and type 1 diabetic mice, using ^{111}In-exendin-3. In **Chapter 1**, an overview is provided about the current state-of-the-art in radionuclide imaging of islet grafts and the use of small animal models for characterizing novel β-cell radiotracers. In **Chapter 2**, the role of islet graft revascularization for *in vivo* delivery of ^{111}In-exendin to the islets was determined by follow-up of ^{111}In-exendin-3 accumulation by the islets during the first weeks after transplantation. In this Chapter, we determined the optimal time-point after which reproducible (quantitative) imaging of islet grafts can be achieved. In **Chapter 3**, we studied the correlation between exendin accumulation and the BCM in transplants containing various amounts of islets (50 to 800 islets). In **Chapter 4**, we evaluated the possibility for *in vivo* monitoring of islet transplants in diabetic recipients where islet grafts underwent severe hyperglycemic stress. Finally, we described in **Chapter 5** a multi-modal imaging approach for fast and reliable cross-examination of ^{111}In-exendin performances in BCM assessment.

References

1. *IDF Diabetes Atlas, 7 ed., Brussels Belgium: International Diabetes Federation.* 2015.
2. Shapiro , A.M.J., et al., *Islet Transplantation in Seven Patients with Type 1 Diabetes Mellitus Using a Glucocorticoid-Free Immunosuppressive Regimen.* New England Journal of Medicine, 2000. **343**(4): p. 230-238.
3. Shapiro, A.M.J., et al., *Islet Transplantation in Seven Patients with Type 1 Diabetes Mellitus Using a Glucocorticoid-Free Immunosuppressive Regimen.* New England Journal of Medicine, 2000. **343**(4): p. 230-238.
4. Ryan, E.A., et al., *Five-Year Follow-Up After Clinical Islet Transplantation.* Diabetes, 2005. **54**(7): p. 2060-2069.
5. Biarnés, M., et al., β-Cell Death and Mass in Syngeneically Transplanted Islets Exposed to Short- and Long-Term Hyperglycemia. Diabetes, 2002. **51**(1): p. 66-72.
6. Lee, Y., et al., *Metabolic Mechanisms of Failure of Intraportally Transplanted Pancreatic* β*-Cells in Rats: Role of Lipotoxicity and Prevention by Leptin.* Diabetes, 2007. **56**(9): p. 2295-2301.
7. Meier, J.J. and R.C. Bonadonna, *Role of Reduced* β*-Cell Mass Versus Impaired* β*-Cell Function in the Pathogenesis of Type 2 Diabetes.* Diabetes Care, 2013. **36**(Supplement 2): p. S113-S119.
8. Sherry, N.A., E.B. Tsai, and K.C. Herold, *Natural History of* β*-Cell Function in Type 1 Diabetes.* Diabetes, 2005. **54**(suppl 2): p. S32-S39.
9. Brom, M., et al., *Non-invasive quantification of the beta cell mass by SPECT with 111In-labelled exendin.* Diabetologia, 2014. **57**(5): p. 950-959.
10. Brom, M., et al., *Radiolabelled GLP-1 analogues for in vivo targeting of insulinomas.* Contrast media & molecular imaging, 2012. **7**(2): p. 160-166.
11. Gotthardt, M., et al., *Use of the incretin hormone glucagon-like peptide-1 (GLP-1) for the detection of insulinomas: initial experimental results.* European Journal of Nuclear Medicine and Molecular Imaging, 2002. **29**(5): p. 597-606.
12. Wu, Z., et al., *Development and evaluation of 18F-TTCO-Cys40-Exendin-4: a PET probe for imaging transplanted islets.* J Nucl Med, 2013. **54**(2): p. 244-51.
13. Pattou, F., J. Kerr-Conte, and D. Wild, *GLP-1-receptor scanning for imaging of human beta cells transplanted in muscle.* N Engl J Med, 2010. **363**(13): p. 1289-90.

2

General introduction

1. Role of imaging in islet transplantation

Diabetes mellitus is a group of metabolic disorders characterized by long-standing hyperglycemia. In type 1 diabetes (T1D), the inability in maintaining normoglycemia results from auto-immune destruction of the β-cells and consequently, insulin-dependency. In type 2 diabetes (T2D), hyperglycemia results from resistance to insulin by the hormone target cells (namely myocytes and adipocytes) in association with insufficient insulin secretory response.

The auto-immune form of diabetes accounts for 5–10% of diabetes patients [1]. Several events occur before the clinical onset of T1D, and our current understanding of the disease is largely based on small animal models that spontaneously develop diabetes (e.g. NOD mice): Genetic predisposition is a key component in the first steps of disease development, where several HLA alleles, polymorphism in the insulin promoter region, and multiple loci that are involved in the regulation of the immune-system were identified as risk factors [2]. Environmental factors might also be involved in priming the auto-immune assaults, such as enteroviruses, infections and the interaction of intestinal bacteria with the mucosal immune cells [3, 4]. The combination of environmental factors with the T1D pre-disposing loci triggers insulitis (β-cell-directed auto-immune assaults). Insulitis results in specific destruction of β-cells, which leads to production of autoantibodies to insulin and, at later stages, autoantibodies to for example glutamic acid decarboxylase (GAD_{65}), β-cell specific Zinc transporter (ZnT8) and to the tyrosine phosphatases (IA-2 and IA-2β). Progressive β-cell loss eventually renders the individual insulin dependent.

The type 2 form of diabetes accounts for most cases of diabetes mellitus, corresponding to 90-95% of the diabetic individuals [5]. Among the multiple environmental causes of T2D, obesity is the major player in disease progression [6]. Genetic factors associated with β-cell dysfunction are also evident [7, 8]. Hyperglycemia occurs gradually and therefore, the disease usually remains unnoticed for a long period, which disposes the individual to vascular complications that increase over-time. The inability of the β-cell to compensate for insulin resistance leads to progressive β-cell failure associated with decreased insulin production, and to a lesser extent, reduction in BCM, resulting in loss of glycemic control and the need for medication.

In T1D patients, a daily insulin injection is the conventional approach to maintain homeostasis of blood glucose levels (90-110 mg/dl, or 4-6 mmol/L). This method is however associated with several disadvantages, where frequent episodes of hypoglycemia and overall poor blood glucose control are the most common ones. Therefore, insulin-dependent patients remain at risk of developing long-term diabetes complications [9].

Since the establishment of the Edmonton protocol [10], transplantation of deceased donor islets in T1D patients has become a promising approach to reverse hyperglycemia in an experimental setting, for individuals who suffer from brittle diabetes and hypoglycemic unawareness [11-13]. Using the Edmonton protocol, islets are obtained from multiple donors and are transplanted in diabetic recipients using glucocorticoid-free immunosuppression regimen.

The isolation procedure consists of (1) enzymatic digestion of the pancreas in order to separate the endocrine tissue (islets containing the β-cells) from the exocrine tissue, (2) purifying the islets by discarding as much exocrine tissue as possible and (3) resting the islets in an appropriate culture medium prior to transplantation [14]. After transplantation and complete engraftment of the islets to the host surrounding tissue, the graft secretes insulin in the blood stream of the recipient in response to elevated blood glucose levels. The successful intra-portal islet transplantation has made the liver the site of choice [12]. The major advantage of islet transplantation is to ensure better control on blood glucose levels, thereby reducing risks of hypoglycemia, and long-term complications.

Islets are, however, lost in large amounts shortly after transplantation, but also on the long-term there are several obstacles that must be addressed to improve the clinical outcome [15]. For instance, the presence of the islets in the hepatic vascular system triggers an instant blood-mediated inflammatory reaction (IBMIR) which compromises islet engraftment, blood supply, and survival [16, 17]. Other factors such as islet lipo/gluco-toxicity are involved in long-term graft failure [15, 18]. The excessive use of immune-suppression drugs for maintaining immune tolerance towards the islets could cause islet toxicity [19, 20]. On the other hand, insufficient immune-suppression could lead to failure in maintaining immune-tolerance and destruction of the graft. Currently, functional and immunological assays are deployed in the clinics to monitor graft function (e.g. measurement of glycemia, C-peptide levels) and to detect anti–β-cell immune attacks (e.g. measurement of anti-HLA antibodies) after islet transplantation [21]. However, both impaired islet function and/or β-cell death can be involved in graft failure, and the current clinical tests are not suited to discriminate between β-cell loss and dysfunction. Furthermore, the parameters measured by these tests have poor predictive value of graft damage [22]. Overall, islet transplantation still exhibits poor clinical long-term outcome [23].

A non-invasive method to quantify graft survival is therefore warranted, not only for early detection of β-cell loss, but also to facilitate development of novel treatment approaches and therapy adaptation to preserve a functional islet graft. In an ideal setting, quantification of BCM should be correlated with clinical functional tests for providing clinicians with comprehensive information about islet graft state (i.e. survival and function). Radioactive imaging modalities such as PET and SPECT offer high detection sensitivity of radioactive probes and are therefore of particular interest

for β-cell imaging. First attempts to image islet grafts were performed using genetically modified islets that express the herpes simplex virus type 1 thymidine kinase (sr39tk). The enzyme phosphorylates radiolabeled thymidine analogues, leading to metabolic trapping inside the β-cells and subsequent detection by PET. Using this strategy, islet grafts could be visualized by a small-animal PET after injection of the sr39tk substrate [^{18}F]-FHBG, allowing for the long-term monitoring of islet transplants [24]. Similarly, islets genetically modified into co-expressing sr39tk and viral interleukin-10 genes, could be visualized by PET while being protected from immune-assaults by modulating the local immune system [25]. Although these studies have demonstrated the value of Nuclear Medicine Imaging for the sensitive visualization of islet grafts, the presented approaches require genetic modification of the islets, which limits their clinical potential.

More recently, islets were pre-labeled with 2-[^{18}F] fluoro-2deoxy-D-glucose (FDG), which allowed for the detection of intra-portally transplanted islets by PET in a rat model as well as in diabetic subjects [26, 27]. However, the short half-life of the F-18 and temporary trapping of the probe within the islets, limits the use of the method for longitudinal follow-up of islet mass. In other studies, non-invasive *in vivo* targeting of β-cell surface markers with radiolabeled peptides, small molecules, antibodies and antibody fragments allowed for the detection of islet transplants in animal models and in humans [28, 29].

The most likely radionuclide-based imaging strategy to be translated into clinics relies on injection of radiolabeled molecular tracers that target β-cell surface markers. The presented approach does not involve genetic manipulation of the islets prior to transplantation and is not limited by the half-life of the radionuclide, since the radiotracer can be injected any time prior to imaging. In the following section, we describe *in vivo* strategies to characterize β-cell radiotracers for *in vivo* quantification of BCM.

2. Validation of novel β-radiotracers

The importance of β-cell mass quantification in islet grafts has triggered intensive preclinical research to develop non-invasive imaging techniques that can be safely implemented into the clinics. Hence, small animal models were widely used to evaluate the clinical potential of new β-cell radiotracers to monitor islet grafts. Mice and rats are convenient models, as they serve as islet donors and recipients, for validation of radiotracers in imaging islet grafts under normal and pathophysiological conditions (e.g. hyperglycemia, lipotoxicity, hypoxia, immune assaults).

Ideally, radiotracer uptake should only be dependent on the number of living β-cells, and expression of the radiotracer target receptor in the islets should not be

significantly influenced by β-cell stress (caused by pathophysiological conditions mentioned above). Changes in tracer uptake due to β-cell stress could lead to erroneous conclusions with regard to the BCM.

For initial investigation of the potential of the radiotracer in quantifying BCM, syngeneic models can be used, where various amounts of islets are transplanted and compared to tracer uptake in healthy (normoglycemic) recipients. The advantage of this approach is that validation of the radiotracer for BCM assessment would not be influenced by confounding factors, such as immune assaults and hyperglycemia, etc.

To investigate the potential of the radiotracer in imaging islet grafts during hyperglycemic events, diabetic recipients should be used. Several chemicals to induce diabetes can be put into use but the two most commonly used compounds are alloxan and streptozotocin (STZ). Both compounds have a structure similar to glucose, therefore, they compete with the glucose present in the body and accumulate in the β-cells, leading to their destruction. It is possible to induce diabetes in most strains of rats and mice, although the sensitivity for the chemicals differs per strain [30]. In these models, a high percentage of the β-cells is destroyed, resulting in hyperglycemia. The amount of β-cells destroyed by the compounds is dependent on the administrated dose, giving us the advantage of controlling the level of BCM in the pancreas, and consequently, the severity of hyperglycemia. After administration of the chemical it takes 5 to 7 days to reach stable hyperglycemia. Destruction of the β-cells in the pancreas of the recipients using these compounds under different doses therefore allows to generate diabetic recipients, where islets can be transplanted and studied for radiotracer uptake during mild or severe hyperglycemic events.

Allo-transplantation and xenotransplantation models can be used to verify if the radiotracer can detect changes in BCM during immune-rejection. Rejection of the islets occurs between 10-14 days after transplantation, where most of islet cells are destroyed [31]. Hence, imaging of islet grafts at different time-points after transplantation could validate the use of a radiotracer in monitoring BCM prior to, during and after immune rejection where partial or complete loss of the graft has occurred.

3. Suitable transplantation sites for Nuclear Medicine Imaging of islet grafts

In contrast to the clinical setting, in small animal models, islets are transplanted at a variety of sites for islet graft imaging with radiotracers. These transplantation sites are chosen based on the following criteria: they should exhibit an environment that allows β-cell survival and proper function. They should offer an environment with high signal-to-background ratio for easy visualization and quantification of tracer uptake by the islets. The background signal can result from the preferred excretion routes of the radiotracer or the expression of the target receptor in the organs of the recipient. Finally, the transplantation site should allow easy histological evaluation of complete transplants (typically by stereological approach), for accurate correlation of tracer uptake with the graft volume that is determined by the area of β-cell markers (e.g. insulin, nkx6.1, pdx1). Typically, fast and accurate histological evaluation of BCM can be achieved when islets are engrafted in a small area rather than being scattered across the transplantation site.

Imaging of human islets transplanted in the liver using ^{64}Cu-labelled exendin was achieved in NOD/SCID mice [28]. Animals transplanted with the islets showed higher PET signal in the whole liver when compared to the control group, demonstrating the potential of this strategy for imaging of intraportally transplanted islets.

The skeletal muscle was previously used as a clinical transplantation site to accommodate islet transplants and reverse hyperglycemia [29, 32, 33]. The organ has high angiogenic potential allowing the establishment of intra-islet blood flow that is comparable to the native environment of pancreatic islets [33]. The transplantation procedure is minimally invasive and relatively easy to perform. Furthermore, the islets can be transplanted in muscle tissues located far away from the radiotracer excretion routes (e.g. renal excretion) and organs that are known to express the target receptor. Finally, easy *in vivo* quantification of tracer uptake and fast histological analysis of complete transplants in preclinical studies is possible, due to the focal engraftment in the muscle. Using this model, islet imaging was achieved by ^{111}In-exendin in a clinical case, where islet mediated uptake of the tracer was clearly visualized by SPECT planar projections [34].

The subcutaneous space has been used for islet transplantation in humans given its easy accessibility and the safety of the procedure. However, the site exhibits low angiogenic potential, which represents an obstacle for proper graft survival and functioning. The large availability of subcutaneous spaces and the possibility to transplant islets into a small distribution area offer similar advantages as described above for the skeletal muscle. Using this model, previous studies demonstrated that human islets transduced with the simplex virus type 1 thymidine kinase (HSV1-tk) can be targeted *in vivo* with [^{18}F]FHBG and visualized by PET in mice [24].

4. Background and aims of the thesis

The glucagon-like peptide-1 (GLP-1) receptor is a promising target receptor for β-cell imaging [35]. It is a G-protein coupled receptor, which internalizes the endogenous ligand GLP-1 after binding. Since GLP-1 is quickly degraded by dipeptidyl peptidase-4 (DPP-4) in the blood [36] and has a half-life time that is less than 2 minutes [37], stable GLP-1 analogues are used to target the GLP-1R, such as exendin-3 and exendin-4 [38-40].

The specificity of radiolabeled exendin towards the β-cells has been a matter of debate. In fact, α-cells were reported to express the receptor [41-43], while in other studies, the GLP-1R was shown to be specific to the β-cells [44-46]. Most importantly, it was demonstrated that ^{111}In-exendin uptake in the pancreas correlates with BCM and not with α-cell mass [47]. It was in fact demonstrated that accumulation of ^{111}In-exendin-3 in the β-cells allows to measure differences in BCM in the pancreas of rat models for diabetes, as well as in healthy and diabetic subjects using SPECT imaging, without apparent interference of the α-cells on the measurements [48].

Non-invasive measurement of the BCM in islet grafts using a similar approach could allow to improve the clinical outcome of islet transplantation. Whether the radiotracer is suitable to quantify BCM after islet transplantation was, however, not yet demonstrated. Moreover, it was previously reported that hyperglycemia could down-regulate the expression of the GLP-1R, which might occur in islet recipients with poorly regulated blood glucose levels [49]. Down-regulation of the GLP-1R could be misleading when measuring the true BCM, using ^{111}In-exendin, and must therefore be investigated.

The aim of this thesis was to characterize the targeting properties of ^{111}In-exendin-3 in transplanted islets and to validate the radiotracer utility for non-invasive quantification of BCM using healthy (control) and diabetic C3H mouse recipients.

References

1. Association, A.D., *Diagnosis and Classification of Diabetes Mellitus.* Diabetes Care, 2008. **31**(Supplement 1): p. S55-S60.
2. Noble, J.A. and H.A. Erlich, *Genetics of Type 1 Diabetes.* Cold Spring Harbor Perspectives in Medicine, 2012. **2**(1).
3. Berg, A.K., O. Korsgren, and G. Frisk, *Induction of the chemokine interferon-gamma-inducible protein-10 in human pancreatic islets during enterovirus infection.* Diabetologia, 2006. **49**(11): p. 2697-2703.
4. Vaarala, O., M.A. Atkinson, and J. Neu, *The "Perfect Storm" for Type 1 Diabetes: The Complex Interplay Between Intestinal Microbiota, Gut Permeability, and Mucosal Immunity.* Diabetes, 2008. **57**(10): p. 2555-2562.
5. Zimmet, P., K.G.M.M. Alberti, and J. Shaw, *Global and societal implications of the diabetes epidemic.* Nature, 2001. **414**(6865): p. 782-787.
6. Fonseca, V.A., *Defining and Characterizing the Progression of Type 2 Diabetes.* Diabetes Care, 2009. **32**(suppl 2): p. S151-S156.
7. Cnop, M., et al., *Progressive Loss of β-Cell Function Leads to Worsening Glucose Tolerance in First-Degree Relatives of Subjects With Type 2 Diabetes.* Diabetes Care, 2007. **30**(3): p. 677-682.
8. Stride Amanda, A.A., *Different genes, different diabetes: lessons from maturity-onset diabetes of the young.* Annals of medicine, 2002. **34**(3): p. 207-16.
9. Melendez-Ramirez, L.Y., R.J. Richards, and W.T. Cefalu, *Complications of Type 1 Diabetes.* Endocrinology and Metabolism Clinics of North America, 2010. **39**(3): p. 625-640.
10. Shapiro , A.M.J., et al., *Islet Transplantation in Seven Patients with Type 1 Diabetes Mellitus Using a Glucocorticoid-Free Immunosuppressive Regimen.* New England Journal of Medicine, 2000. **343**(4): p. 230-238.
11. Ballinger, W.F. and P.E. Lacy, *Transplantation of intact pancreatic islets in rats.* Surgery. **72**(2): p. 175-186.
12. Scharp, D.W., et al., *Insulin Independence After Islet Transplantation Into Type I Diabetic Patient.* Diabetes, 1990. **39**(4): p. 515-518.
13. Shapiro, A.M.J., et al., *Portal Vein Immunosuppressant Levels and Islet Graft Toxicity.* Transplantation Proceedings, 1998. **30**(2): p. 641.
14. Carter, J.D., et al., *A Practical Guide to Rodent Islet Isolation and Assessment.* 2009. **11**: p. 3-31.
15. Biarnés, M., et al., β-Cell Death and Mass in Syngeneically Transplanted Islets Exposed to Short- and Long-Term Hyperglycemia. Diabetes, 2002. **51**(1): p. 66-72.
16. Nilsson, B., K.N. Ekdahl, and O. Korsgren, *Control of instant blood-mediated inflammatory reaction to improve islets of Langerhans engraftment.* Current Opinion in Organ Transplantation, 2011. **16**(6): p. 620- 626.
17. Moberg, L., et al., *Production of tissue factor by pancreatic islet cells as a trigger of detrimental thrombotic reactions in clinical islet transplantation.* The Lancet. **360**(9350): p. 2039-2045.
18. Lee, Y., et al., *Metabolic Mechanisms of Failure of Intraportally Transplanted Pancreatic β-Cells in Rats: Role of Lipotoxicity and Prevention by Leptin.* Diabetes, 2007. **56**(9): p. 2295-2301.
19. Campbell, P.M., et al., *High Risk of Sensitization After Failed Islet Transplantation.* American Journal of Transplantation, 2007. **7**(10): p. 2311-2317.
20. Barlow, A.D., M.L. Nicholson, and T.P. Herbert, *Evidence for Rapamycin Toxicity in Pancreatic β-Cells and a Review of the Underlying Molecular Mechanisms.* Diabetes, 2013. **62**(8): p. 2674-2682.
21. Roep, B.O., et al., *Auto- and alloimmune reactivity to human islet allografts transplanted into type 1 diabetic patients.* Diabetes, 1999. **48**(3): p. 484-490.
22. Pileggi, A., et al., *Factors influencing Islet of Langerhans graft function and monitoring.* Clinica Chimica Acta, 2001. **310**(1): p. 3-16.
23. Ryan, E.A., et al., *Five-Year Follow-Up After Clinical Islet Transplantation.* Diabetes, 2005. **54**(7): p. 2060- 2069.
24. Lu, Y., et al., *Long-Term Monitoring of Transplanted Islets Using Positron Emission Tomography.* Mol Ther, 2006. **14**(6): p. 851-856.
25. Kim, S.-J., et al., *Quantitative micro positron emission tomography (PET) imaging for the in vivo determination of pancreatic islet graft survival.* Nat Med, 2006. **12**(12): p. 1423-1428.

26. Toso, C., et al., *Positron-Emission Tomography Imaging of Early Events after Transplantation of Islets of Langerhans.* Transplantation, 2005. **79**(3): p. 353-355.
27. Eich, T., et al., *Positron Emission Tomography: A Real-Time Tool to Quantify Early Islet Engraftment in a Preclinical Large Animal Model.* Transplantation, 2007. **84**(7): p. 893-898.
28. Wu, Z., et al., *Development and evaluation of 18F-TTCO-Cys40-Exendin-4: a PET probe for imaging transplanted islets.* J Nucl Med, 2013. **54**(2): p. 244-51.
29. Pattou, F., J. Kerr-Conte, and D. Wild, *GLP-1–Receptor Scanning for Imaging of Human Beta Cells Transplanted in Muscle.* New England Journal of Medicine, 2010. **363**(13): p. 1289-1290.
30. Deeds, M.C., et al., *Single dose streptozotocin-induced diabetes: considerations for study design in islet transplantation models.* Laboratory Animals, 2011. **45**(3): p. 131-140.
31. Evgenov, N.V., et al., *In Vivo Imaging of Immune Rejection in Transplanted Pancreatic Islets.* Diabetes, 2006. **55**(9): p. 2419-2428.
32. *Striated Muscle as Implantation Site for Transplanted Pancreatic Islets.* Journal of Transplantation, 2011.
33. Christoffersson, G., et al., *Clinical and Experimental Pancreatic Islet Transplantation to Striated Muscle: Establishment of a Vascular System Similar to That in Native Islets.* Diabetes, 2010. **59**(10): p. 2569-2578.
34. Pattou, F., J. Kerr-Conte, and D. Wild, *GLP-1-receptor scanning for imaging of human beta cells transplanted in muscle.* N Engl J Med, 2010. **363**(13): p. 1289-90.
35. Tornehave, D., et al., *Expression of the GLP-1 Receptor in Mouse, Rat, and Human Pancreas.* Journal of Histochemistry & Cytochemistry, 2008. **56**(9): p. 841-851.
36. Albrechtsen, N.J.W., et al., *Targeting the intestinal L-cell for obesity and type 2 diabetes treatment.* Expert Review of Endocrinology & Metabolism, 2014. **9**(1): p. 61-72.
37. Deacon, C.F., et al., *Both Subcutaneously and Intravenously Administered Glucagon-Like Peptide I Are Rapidly Degraded From the NH₂-Terminus in Type II Diabetic Patients and in Healthy Subjects.* Diabetes, 1995. **44**(9): p. 1126.
38. Andralojc, K., et al., *In vivo visualization of transplanted islets in rats by SPECT with In-111-Exendin-3.* J NUCL MED MEETING ABSTRACTS, 2011. **52**(1_MeetingAbstracts): p. 467-.
39. Brom, M., et al., *Non-invasive quantification of the beta cell mass by SPECT with 111In-labelled exendin.* Diabetologia, 2014. **57**(5): p. 950-959.
40. Wang, Y., et al., *Synthesis and evaluation of [18F]exendin (9–39) as a potential biomarker to measure pancreatic β-cell mass.* Nuclear Medicine and Biology, 2012. **39**(2): p. 167-176.
41. De Marinis, Y.Z., et al., *GLP-1 inhibits and adrenaline stimulates glucagon release by differential modulation of N- and L-type Ca2+ channel-dependent exocytosis.* Cell Metab, 2010. **11**(6): p. 543-53.
42. Heller, R.S., T.J. Kieffer, and J.F. Habener, *Insulinotropic glucagon-like peptide I receptor expression in glucagon-producing alpha-cells of the rat endocrine pancreas.* Diabetes, 1997. **46**(5): p. 785-91.
43. Orskov, C. and S.S. Poulsen, *Glucagonlike peptide-I-(7-36)-amide receptors only in islets of Langerhans. Autoradiographic survey of extracerebral tissues in rats.* Diabetes, 1991. **40**(10): p. 1292-6.
44. Tornehave, D., et al., *Expression of the GLP-1 receptor in mouse, rat, and human pancreas.* J Histochem Cytochem, 2008. **56**(9): p. 841-51.
45. Horsch, D., et al., *Reciprocal cellular distribution of glucagon-like peptide-1 (GLP-1) immunoreactivity and GLP-1 receptor mRNA in pancreatic islets of rat.* Pancreas, 1997. **14**(3): p. 290-4.
46. Moens, K., et al., *Expression and functional activity of glucagon, glucagon-like peptide I, and glucose-dependent insulinotropic peptide receptors in rat pancreatic islet cells.* Diabetes, 1996. **45**(2): p. 257-61.
47. Brom, M., et al., *(111)In-exendin uptake in the pancreas correlates with the beta-cell mass and not with the alpha-cell mass.* Diabetes, 2015. **64**(4): p. 1324-8.
48. Brom, M., et al., *Non-invasive quantification of the beta cell mass by SPECT with (1)(1)(1)In-labelled exendin.* Diabetologia, 2014. **57**(5): p. 950-9.
49. Rajan, S., et al., *Chronic hyperglycemia downregulates GLP-1 receptor signaling in pancreatic β- cells via protein kinase A.* Molecular Metabolism, 2015. **4**(4): p. 265-276.

3

Graft revascularization is essential for non-invasive monitoring of transplanted islets with radiolabeled exendin

AUTHORS: ETER W.A., BOS D., FRIELINK C., BOERMAN O.C., BROM M. & GOTTHARDT M.

Department of Radiology and Nuclear Medicine, Radboud University Medical Center, Nijmegen, The Netherlands.

Adapted from: *Scientific Reports* **5**, 15521, doi:10.1038/srep15521 (2015).

Abstract

Islet transplantation is a novel promising strategy to cure type 1 diabetes. However, the long-term outcome is still poor, because both function and survival of the transplant decline over-time. Non-invasive imaging methods have the potential to enable monitoring of islet survival after transplantation and the effects of immunosuppressive drugs on transplantation outcome. ^{111}In-labeled exendin-3 is a promising tracer to visualize native and transplanted islets by SPECT (Single Photon Emission Computed Tomography). In the present study, we hypothesized that islet microvasculature plays an important role determining the uptake of exendin-3 in islets when monitoring transplant survival. We observed ^{111}In-exendin-3 accumulation in the transplant as early as three days after transplantation and an increase in the uptake up to three weeks post-transplantation. Islet-revascularization correlated with the increase of uptake of ^{111}In-exendin-3, whereas fully re-established islet vasculature coincided with a stabilized uptake of the radiotracer in the transplant. Here, we demonstrate the importance of islet vasculature for *in vivo* delivery of radiotracers to transplanted islets and we demonstrate that optimal and stable uptake of exendin four weeks after transplantation opens the possibility for long-term monitoring of islet survival by SPECT imaging.

Introduction

Reversal of type 1 diabetes by transplanting pancreatic islets has emerged as a promising therapeutic approach [1, 2]. However, insulin independence shows a rapid decrease and can hardly be preserved beyond 5 years after the intervention [3]. Moreover, several studies reported impaired islet survival after liver transplantation, which was caused by insufficient revascularization [4] and triggering of blood-mediated inflammatory reactions [5], along with lipo and/or gluco-toxicity [6-8].

Current functional tests cannot determine whether graft failure is caused by functional impairment of β-cells or β-cell loss, as many factors can be involved in this process (i.e. immune rejection, decline in islet function through metabolic or inflammatory stress) [3, 9]. Biomedical imaging techniques can therefore be used to monitor islet survival in addition to islet function measured by clinical testing and can therefore contribute to future clinical decision making regarding treatment assignment or adaptation. Pre-labeling of islets with super-paramagnetic iron oxide particles (SPIOs) for MR imaging of islet transplants has been introduced a decade ago [10]. Further studies demonstrated that human islets transplanted in rodents can be monitored and quantified by MRI up to 6 months post-transplantation [11]. Labeling of the islets with SPIOs prior to transplantation is therefore a promising technique for clinical studies [12].

In other studies, radioactive-based imaging methods were used for their advanced detection sensitivity of *in vivo* tracer uptake by transplanted or native islets [13, 14]. In particular, SPECT imaging after injection of ^{111}In-labeled exendin was reported as a promising strategy to non-invasively visualize engrafted islets, as well as to visualize and quantify BCM in the pancreas of healthy and diabetic subjects [15, 16]. Therefore, this tracer could be suitable for repeated longitudinal clinical imaging of islet transplants. The advantage of the tracer is the ability of repeated scanning without requiring pre-labeling of the islets prior to transplantation. However, the targeting properties of the radiotracer to the islet grafts early after transplantation may depend on the vasculature that is disrupted after islet isolation [17-19].

Imaging of islet grafts in the skeletal muscle has been demonstrated previously [16], and allows monitoring of the transplant since the islets remain localized in a small engraftment area, where specific uptake can be easily discriminated from the surrounding tissue. Making use of this transplantation model, we determined the correlation between islet graft revascularization and the uptake of ^{111}In-exendin-3 in the transplant for several weeks following islet transplantation.

Research Design and Methods

Animals. Female C3H/HeNCrl mice (22–30 g) were purchased from Charles River (Calco, Italy). All experiments were conducted in accordance with Radboud University guidelines on humane care and use of laboratory animals, and were approved by the Animal Ethical Committee of the Radboud University, Nijmegen, The Netherlands.

Pancreatic islet isolation and transplantation. Pancreatic islets were isolated from 8 weeks-old female C3H/HeNCrl mice by collagenase digestion method. Mice were euthanized and 2 ml of cold RPMI 1640 (Invitrogen, Carmarillo, CA, USA) containing collagenase-V (0.9 mg/ml, Sigma Aldrich, St Louis, MO, USA) was infused via the pancreatic duct. Pancreata were collected in RPMI medium with collagenase and were digested at 37°C for 12 min. The digested tissue was washed twice in RPMI medium and was filtered through a 500 μm filter to separate the islets from undigested tissues. Islets purification was performed on a discontinuous Ficoll gradient (1.118, 1.096 and 1.037 g/ml, Cellgro by Mediatech Inc., Manassas, VA, USA), respectively, and centrifuged at 625 x g for 16 min without brake. Islets were collected from the aqueous phase between the first and second layer and washed twice with RPMI medium. Finally, islets were incubated overnight in a humidified 5% CO_2 atmosphere at 37°C in RPMI 1640 medium containing L-glutamine (Sigma), penicillin-streptomycin (10 mg/ml, Sigma Aldrich) and 10% v/v fetal calf serum (HyClone, Celbio, Logan, UT, USA). Islets were counted and hand-picked under a bright field microscope. Eight hundred islets were transferred to an eppendorf tube and centrifuged at 62 x g for 2 minutes and aspirated in a canula by a Hamilton syringe. Syngenic transplantation was performed in the calf muscle, parallel to the fibula, using needles with a 0.8 mm diameter. To determine the exact number of transplanted islets, the canula was washed with fresh medium which was collected in the eppendorf tube used for preparation of the islets. The exact number of transplanted islets was determined by subtracting the remaining islets in the tube from the initially counted number.

Radiolabeling of exendin-3. [Lys^{40}(DTPA)]-exendin-3 was purchased from Peptide Specialty Laboratories (Heidelberg, Germany). Peptide labeling with In-111 was performed as previously described [15]. Radiochemical purity was determined by ITLC and radiolabeled exendin-3 was purified by solid-phase extraction using a HLB-cartridge (Waters, Etten-Leur, The Netherlands) prior to animal injection as previously reported [15]. All animals were injected with 0.1 μg of exendin-3 corresponding to approximately 15 MBq.

Binding assay on isolated islets. The binding of radiolabeled exendin-3 to islets was examined on isolated islets from C3H mice. After overnight recovery from

isolation procedure, islets were collected and the medium was removed by centrifugation as described above. The islets were diluted in binding buffer (RPMI 1640 containing 0.5% BSA (w/v)) and 100 or 300 islets (triplicate) were added to 24-transwell plates (Corning B.V. Life Sciences, Amsterdam, The Netherlands) and counted under a bright-field microscope (Meyer Instruments, Huston TX, USA). The islets were washed with 200 μl of binding buffer and 1.5 fmol of In-111-exendin-3 in 200 μl of binding buffer were added. Excess of unlabeled exendin-3 (corresponding to 0.62 nmol) was added to 3 additional wells per condition to examine GLP-1R mediated binding. After 4 h incubation at 37°C the islets were washed twice with binding buffer, the transwells containing the islets were measured in a γ-counter (Wallac 1480 Wizard, Perkin Elmer, Boston, MA, USA) and the bound fraction was determined.

Imaging procedure and data acquisition. Mice were injected intravenously with 15 MBq of exendin-3 and were scanned 1 hour after injection. Scans were performed with a small animal U-SPECT-II/CT system (MILabs, Utrecht, The Netherlands) with a 1 mm multi-pinhole ultra-high sensitivity mouse collimator for 50 minutes. Mice were scanned after 3 days, 1, 2, 3, 4, 5 or 6 weeks post-transplantation. All mice were scanned twice with 7 days difference, under the same parameters. Immediately after the second SPECT acquisition, mice were euthanized and calf muscles containing the transplant were dissected and were put in 4% paraformaldehyde inside eppendorf tubes and were scanned *ex vivo* with the same settings. All images were reconstructed with OSEM (3 iterations, 16 subsets, voxel size 0.4 mm) using the U-SPECT-Rec software (MILabs, Utrecht, The Netherlands). CT scans were performed in full/accurate mode or partial/fast mode under 615 μA/s and 65 kV. For quantification of SPECT images, a volume of interest (VOI) was manually drawn around the observed uptake in the transplantation site and the background was subtracted by using the same VOI applied on the contra-lateral calf muscle, which contained no transplant. Data were corrected for the injected dose and converted to Bq by using external standards with known activity scanned and reconstructed with the same settings.

Histological analyzes. Muscles were fixed in 4% paraformaldehyde and embedded in paraffin after SPECT acquisition. For autoradiography, muscles were sliced into 4 μm sections and were exposed to an imaging plate (Fuji Film BAS-SE 2025, Raytest, Straubenhardt, Germany) for 7 days. Images were visualized with a radioluminography laser imager (Fuji Film BAS 1800 II system, Raytest, Straubenhardt, Germany). Quantitative analysis of the autoradiographical images was performed using AIDA Image Analyzer software (Raytest GmbH, Straubenstadt, Germany). Data were acquired by drawing ROIs around each transplant as well as around the standards with known amount of radioactivity. Subsequently, sections were stained with hema-

toxylin-eosin (HE) to confirm the presence of pancreatic islets. Finally, for immunohistochemical staining of insulin, consecutive sections underwent antigen retrieval for 10 min in 10 mM citrate pH 6 at 96°C and blocked with 1% BSA in PBS for 30 minutes and endogenous peroxidase activity was blocked with 3% H_2O_2 in PBS for 30 minutes. Staining was performed using anti-insulin rabbit antibody (Santa Cruz Biotechnology, Santa Cruz, CA, USA) diluted 1/500 for 2 hours at room temperature. Sections were incubated with swine anti-rabbit conjugated with peroxidase, for 1 hour at room temperature and washed with PBS. The staining was developed with Bright DAB (Immunologic, Duiven, The Netherlands) and sections were visualized under bright-field microscopy. To normalize the autoradiography measurements by the corresponding transplant surface, the outline of insulin-positive cells of consecutive sections was manually drawn in imageJ (data are expressed as Bq/mm^2). To normalize SPECT data by the size of the transplant, the volume was calculated by multiplying the insulin positive surface per level by the distance separating each analyzed section, that is 50 μm. For determination of vascular density, consecutive sections were blocked with 1% BSA in PBS for 30 minutes and stained with anti-insulin guinea-pig antibody (Dako, Heverlee, Belgium) diluted 1/1000 and anti-VEGFR-2 rabbit antibody (Cell signaling, Danvers MA, USA) diluted 1/200 for 2 hours at room temperature. Sections were next incubated with goat anti-guinea pig Alexa 488 (1/200; Life technology, Dallas, TX, USA) and goat anti-rabbit Alexa 594 (1/200; Life technology), respectively, for 1 hour at room temperature. To confirm the expression of the GLP-1R, sections were blocked with 1% BSA in PBS for 30 minutes and stained with anti-GLP-1R rabbit antibody (Abcam, Cambridge, UK) diluted 1/500 for 2 hours at room temperature. Sections were next incubated with goat anti-rabbit Alexa 594 diluted 1/300 for 1 hour at room temperature. Sections were mounted and visualized with an epifluorescence microscope (Axioskop Zeiss, Thornwood, NY, USA).

Statistical analysis. Measurements are given as means ± SEM. Multiple comparisons were analyzed by one-way ANOVA and Bonferroni post-hoc test, P value <0.05 was considered statistically significant. Data processing was performed with Graphpad Prism 5 (GraphPad Software, San Diego, CA, USA). Animals that showed no SPECT signal as well as no histological signs of insulin staining, were excluded from the study.

Results

Radiolabeled exendin-3 binds to the GLP-1R on mouse islets in vitro. Incubation of 1.5 fmol of radiolabeled exendin-3 with 100 islets for 4 hours resulted in the binding of $9.1x10^{-3}$ fmol (fig. 1). Binding of radiolabeled exendin-3 was reduced to $3.3x10^{-3}$ fmol in the presence of excess of unlabeled exendin-3 ($p<0.05$). Binding of radiolabeled exendin-3 was two-fold higher when added to 300 islets ($17.5x10^{-3}$ fmol) and binding was successfully decreased to $3.7x10^{-3}$ fmol by applying an excess of unlabeled exendin-3 ($p<0.001$), which confirmed the expression of the GLP-1R.

Exendin-3 uptake in the skeletal muscle is localized in the transplanted islets. In order to determine whether the uptake of exendin-3 originates from the transplant within the skeletal muscle, we performed *ex vivo* autoradiography of the muscle regions that contain the islets, followed by histochemical staining. As evidenced in figure 2 (A-F), there was accumulation of ^{111}In-exendin-3 within well-localized regions of the muscle after 3 days, 1, 2, 3, 4 and 6 weeks in the islet transplants. Sections were next analyzed by HE staining, where the uptake was confirmed as islet-specific. Immunohistochemical staining of muscle sections with an anti-insulin monoclonal antibody confirmed that the transplant predominantly consisted of β-cells (fig. 2G).

Quantitative analysis of ^{111}In-exendin-3 accumulation within transplanted islets by autoradiography was 0.48 ± 0.068, 0.99 ± 0.16, 1.35 ± 1.08, 2.97 ± 0.27, 2.73 ± 0.4 and 3.45 ± 0.34 Bq/mm^2 at 3 days and 1, 2, 3, 4, 6 weeks after transplantation,

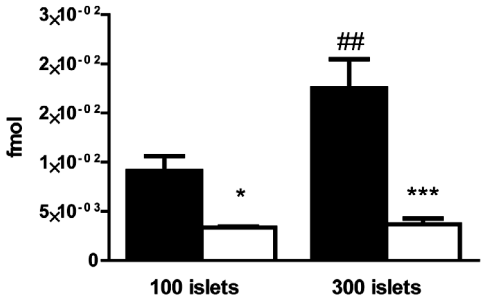

Figure 1 In-vitro binding of radiolabeled exendin-3 to mouse pancreatic islets.

Quantification of radiolabeled exendin-3 (black columns) shows higher binding to 300 islets than to 100 islets. Blocking of the receptor with an excess of unlabeled exendin-3 (white columns) significantly decreased the binding. Data are shown as means ± SEM from 3 experiments. *$p<0.05$, ***$p<0.001$ compared with the corresponding amount of islets, whereas *##p<0.01* compared with 100 islets.

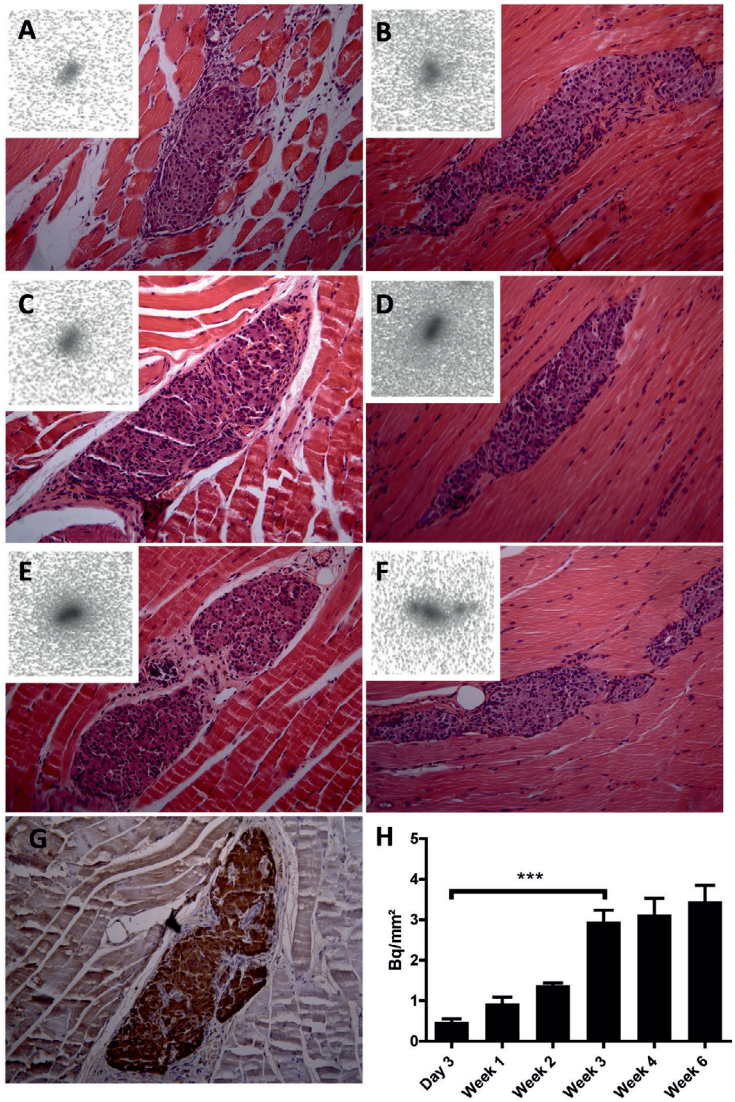

Figure 2 Ex-vivo measurement of exendin-3 uptake by transplanted islets.

(***A-F***) Autoradiography of muscle sections shows hotspots of In-111 accumulation. Histochemical staining of the corresponding autoradiography section shows co-localization between the uptake of exendin-3 and the transplant. (***G***) Adjacent sections were stained with anti-insulin mAb to confirm the presence of β-cells (brown). (***H***) Quantification of In-111 uptake (expressed in becquerel/mm^2) according to autoradiography shows significant increase between 3 days to 3 weeks-old transplants (***$p<0.001$) and stabilized uptake between 3 and 6 weeks post-transplantation.

respectively (fig. 2H). Immunostaining of the GLP-1R with a polyclonal antibody confirmed the expression of the receptor in the transplants (fig. 3).

The density of newly formed blood vessels in the transplant correlates with the uptake of exendin-3. To investigate whether revascularization of transplanted islets affects the uptake of radiolabeled exendin-3, VEGFR-2 and insulin expression was quantified to determine islet microvasculature and β-cells area, respectively (fig. 4). The first vascular structures in the graft were observed 3 days after transplantation. At that time, VEGFR-2 positive endothelial cells were mostly surrounding the transplant (fig. 4A-B).

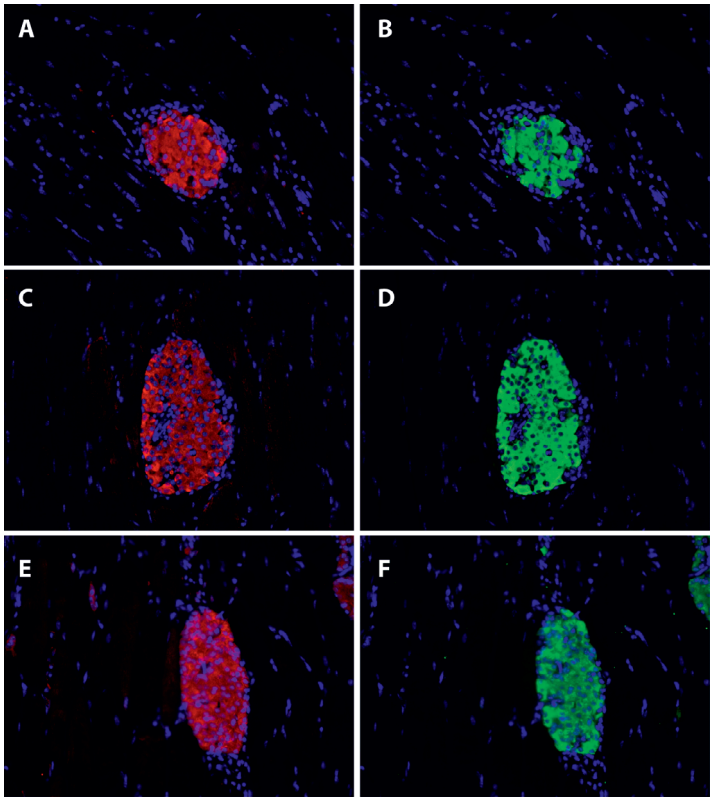

Figure 3 GLP-1R expression is maintained in the islets early after transplantation.

Representative images of 3 days (***A-B***), 2 weeks (***C-D***) and 4 weeks-old transplants (***E-F***) stained for GLP-1R (red) and insulin (green).

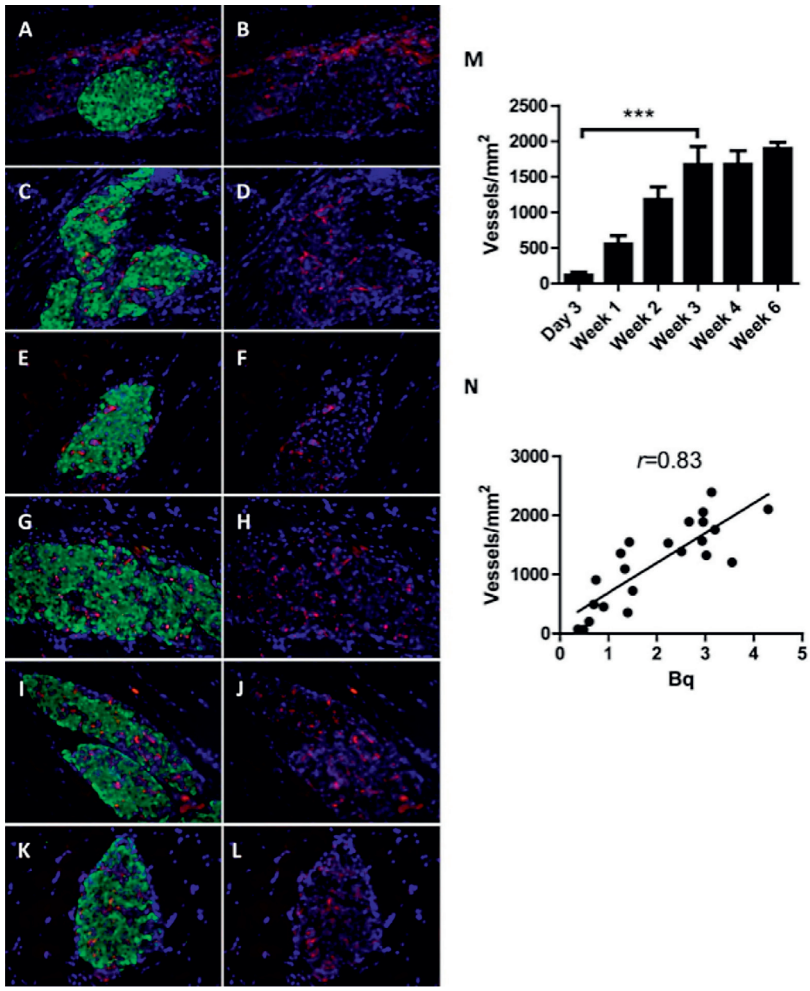

Figure 4 Histological analysis of islet revascularization in the skeletal muscle.

(***A-L***) Representative images of 3 days to 6 weeks-old islet transplants for which β-cells were stained with anti-insulin (green) and the ingrowing VEGFR2-expressing capillaries (red). All sections were counter-stained with DAPI (blue). (***M***) Quantification of vascular density within the insulin positive area shows significant increase in number of vessels from 3 days to 3 weeks (***$p<0.001$). (***N***) Initiation and increase of islet vascular density correlates with increasing exendin-3 uptake (Pearson $r=0.83$). Data are shown as means ± SEM from 4-5 animals.

There was notable progress of angiogenesis one week after transplantation, as more endothelial cells had infiltrated the islets (fig. 4C-D). Intra-islet vasculature was more prominent between 2 weeks and 6 weeks after transplantation, as vessels clearly had penetrated from the periphery into the core of the transplant (fig. 4E-L). Quantitative analysis of revascularization showed notable progress between 3 days and 3 weeks ($p<0.001$) and a stablized vascular density between 3 and 6 weeks (fig. 4M). First signs of revascularization coincided with low exendin-3 uptake by 3-day old grafts and increase in islet vascular density correlated with the uptake of exendin-3 by the islets (Pearson correlation coefficient $r=0.83$) (fig. 4N).

In vivo visualization of islet transplants is dependent on islet revascularization. To assess the correlation between intra-islet vascular density and the tracer concentration in the transplant, SPECT scans were performed at different time-points after transplantation. SPECT visualized 3 days to 6 weeks-old transplants within the skeletal muscle (fig. 5A). After 3 days, 12.5 ± 2.7 kBq/mm^3 accumulated in the transplants, which further increased up to 63 ± 4.7 kBq/mm^3 at 4 weeks and remained similar up to 6 weeks after transplantation (68 ± 3.2 and 67 ± 2.5 kBq/mm^3, for week 5 and 6, respectively) (fig. 5B).

Ex vivo acquisitions were in line with the *in vivo* data, as signal could be detected after 3 days and was increased over time (fig. 6).

To determine the time-point after which multiple imaging sessions result in reproducible assessment of ^{111}In-exendin-3 uptake, each mouse was scanned twice with 7 days of interval, starting 3 days, 1, 2, 3, 4 or 5 weeks after transplantation (fig. 7A). Quantitative analysis revealed an increase in the signal 7 days after the initial scans with stabilization being observed between 3 and 4 weeks-old transplants (fig. 7B). Increase in uptake was independent from the transplant size, since the uptake was normalized by the volume of the transplant. Two transplants which were not visible 3 days or 1 week after transplantation, both became detectable at the time of the second scan.

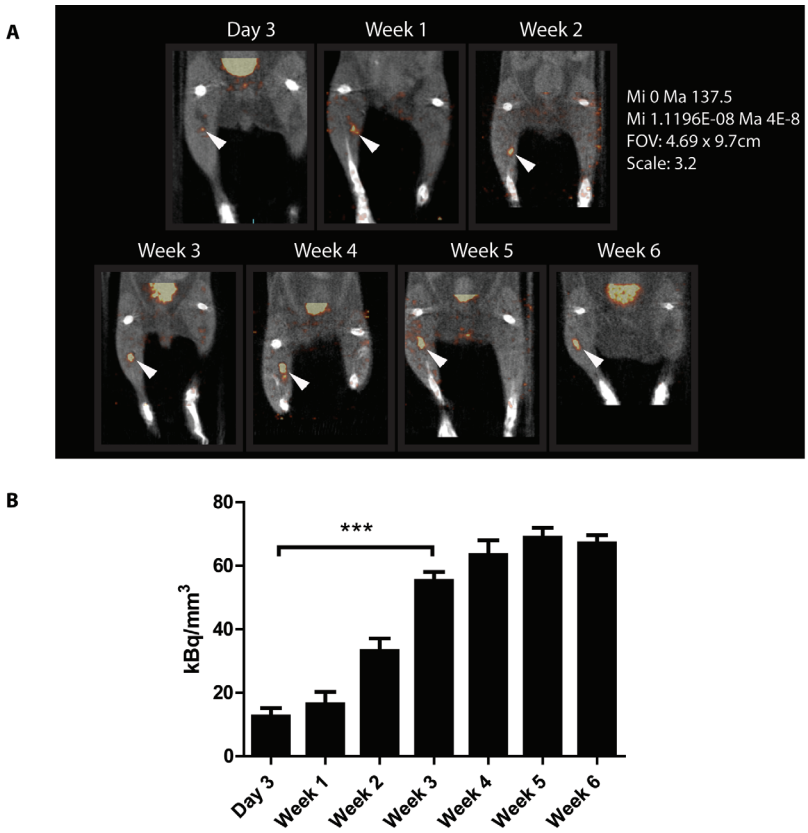

Figure 5 In-vivo detection of pancreatic islets transplanted in the calf muscle.

(***A***) Representative images of C3H mice with transplanted islets. Signal was detected 3 days, 1, 2, 3, 4, 5 and 6 weeks after transplantation (white arrows). (***B***) Quantitative analysis of the SPECT images showed a significant increase in the uptake of ^{111}In-exendin-3 between 3 days and 3 weeks post-transplantation (***$p<0.001$) and a stabilized uptake between 3 and 6 weeks. Data are presented as kBq/mm^3 and are normalized by the injected dose.

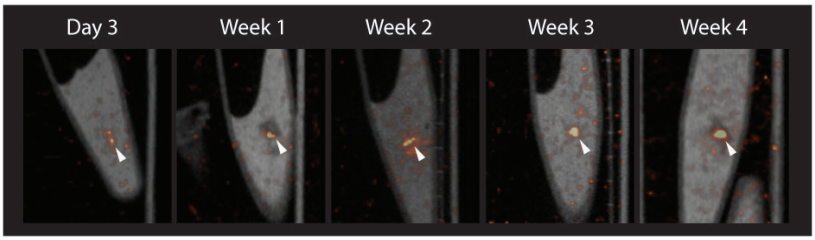

Figure 6 Ex-vivo detection of pancreatic islets transplanted in the calf muscle.

Representative images from *ex-vivo* scans of dissected muscles containing the transplant.

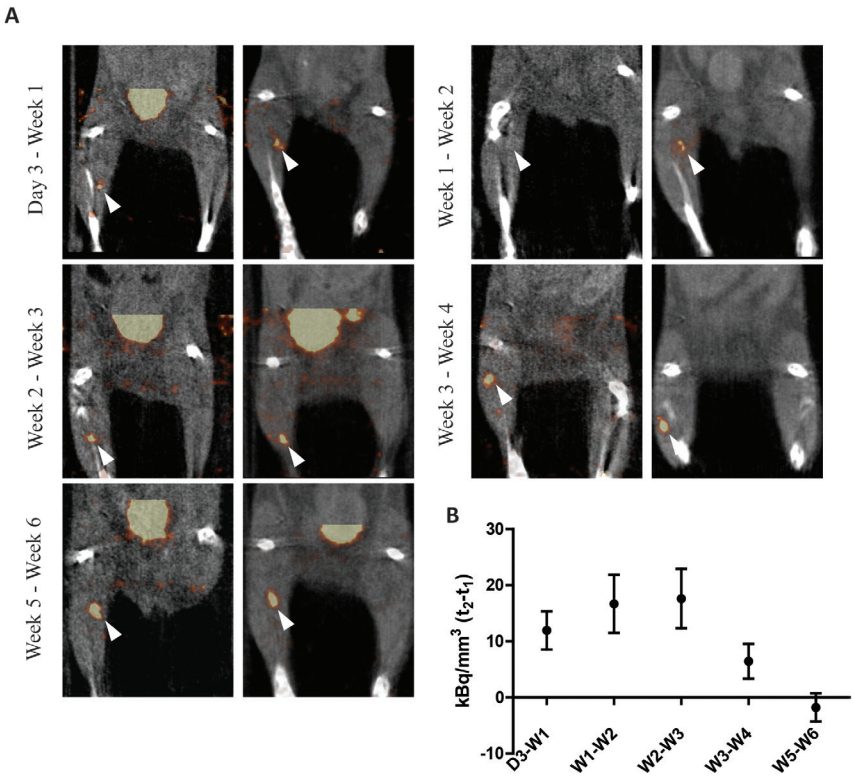

Figure 7 In-vivo detection of pancreatic islets at different weeks.

(***A***) Representative images from *in-vivo* scans at two different time-points with one week interval. Transplants are indicated with white arrows. (***B***) SPECT quantitative analysis where t_2-t_1 corresponds to 7 days interval between both scans shows improved uptake of ^{111}In-exendin-3 and first signs of stabilization of tracer uptake between 3 weeks and 4 weeks post-transplantation.

Discussion

In the present study, we examined the influence of islet graft revascularization on the targeting characteristics of radiolabeled exendin-3, a radiotracer with great potential as imaging biomarker for non-invasive assessment of β-cell survival after transplantation. We demonstrated that an increase in vascular density, between 3 days and 3 weeks after transplantation, correlated with an increase in the accumulation of ^{111}In-exendin-3 in the transplant. Furthermore, in mice in which no signal could be detected three days or one week after transplantation, islet grafts exhibited a detectable uptake at later time-points where vascularity improved. When the vascular bed had been established after 4 weeks, the uptake of exendin-3 indeed stabilized in repeated scans, indicating that islet revascularization has a direct influence on the targeting of transplanted islets after *in vivo* injection of radiotracers. Imaging of islet transplants with radiotracers will therefore reveal reproducible results starting 4 weeks after transplantation, the time-point after which the vascular bed of the transplants appears to have been established.

These findings indicate that recovery of islet vascular network is a prerequisite for reproducible longitudinal evaluation of viable islet grafts. First, complete restoration of islet vasculature improves the transplant signal-to-background ratio which facilitates the quantitative assessment of exendin-3 uptake. Secondly, reproducible uptake of exendin-3 is a requirement to accurately quantify BCM, and changes in the uptake after vasculature has recovered would most likely reflect β-cell loss.

Angiogenesis in recipients with long history of diabetes might be suboptimal [20]. Furthermore, graft angiogenesis rate is dependent on the transplantation site [21]. Therefore, the optimal time-point after which reproducible imaging results are obtained, might be affected by these parameters. The technique will allow, however, to quantify islet survival, months, if not years after transplantation, where failure in maintaining normoglycemia could occur even after successful engraftment of the islets [3].

It was previously reported that islets transplanted in liver can be visualized with small-animal PET, where the uptake of ^{64}Cu-labeled exendin in the liver of transplanted animals was higher as compared to those of the control animals 12 days after transplantation [13]. Here we report the skeletal muscle as a suitable platform for characterization of tracer targeting properties to the islets. Using this model, we could investigate the role of the revascularization of the transplant on radiotracer uptake, since in this model the revascularization could be easily quantified *ex vivo* by histology. This transplantation site could be further used to characterize the targeting properties of novel β-cell radiotracers and to further evaluate existing ones with the advantage of fast histological evaluation of complete transplants.

In conclusion, this study revealed that islet revascularization is a key physiological process when monitoring islet transplants after *in vivo* targeting of the graft with β-cell tracers. Stable and reproducible uptake of exendin was achieved starting 4 weeks after transplantation, indicating that longitudinal assessment of islet survival by SPECT imaging can reproducibly be performed after this time point.

References

1. Thompson, D.M., et al., *Reduced Progression of Diabetic Microvascular Complications With Islet Cell Transplantation Compared With Intensive Medical Therapy.* Transplantation, 2011. **91**(3): p. 373-378.
2. Shapiro, A.M.J., et al., *Islet Transplantation in Seven Patients with Type 1 Diabetes Mellitus Using a Glucocorticoid-Free Immunosuppressive Regimen.* New England Journal of Medicine, 2000. **343**(4): p. 230-238.
3. Ryan, E.A., et al., *Five-Year Follow-Up After Clinical Islet Transplantation.* Diabetes, 2005. **54**(7): p. 2060-2069.
4. Mattsson, G., L. Jansson, and P.-O. Carlsson, *Decreased Vascular Density in Mouse Pancreatic Islets After Transplantation.* Diabetes, 2002. **51**(5): p. 1362-1366.
5. Bennet, W., et al., *Incompatibility between human blood and isolated islets of Langerhans: a finding with implications for clinical intraportal islet transplantation?* Diabetes, 1999. **48**(10): p. 1907-1914.
6. Lee, Y., et al., *Metabolic Mechanisms of Failure of Intraportally Transplanted Pancreatic β-Cells in Rats: Role of Lipotoxicity and Prevention by Leptin.* Diabetes, 2007. **56**(9): p. 2295-2301.
7. Lee, Y., et al., *Beta-cell lipotoxicity in the pathogenesis of non-insulin-dependent diabetes mellitus of obese rats: impairment in adipocyte-beta-cell relationships.* Proceedings of the National Academy of Sciences, 1994. **91**(23): p. 10878-10882.
8. Biarnés, M., et al., β-Cell Death and Mass in Syngeneically Transplanted Islets Exposed to Short- and Long-Term Hyperglycemia. Diabetes, 2002. **51**(1): p. 66-72.
9. Ritzel, R.A., et al., *Relationship Between β-Cell Mass and Fasting Blood Glucose Concentration in Humans.* Diabetes Care, 2006. **29**(3): p. 717-718.
10. Jirák, D., et al., *MRI of transplanted pancreatic islets.* Magnetic Resonance in Medicine, 2004. **52**(6): p. 1228-1233.
11. Evgenov, N.V., et al., *In vivo imaging of islet transplantation.* Nat Med, 2006. **12**(1): p. 144-8.
12. Saudek, F., et al., *Magnetic Resonance Imaging of Pancreatic Islets Transplanted Into the Liver in Humans.* Transplantation, 2010. **90**(12): p. 1602-1606.
13. Wu, Z., et al., *In Vivo Imaging of Transplanted Islets with 64Cu-DO3A-VS-Cys40-Exendin-4 by Targeting GLP-1 Receptor.* Bioconjugate Chemistry, 2011. **22**(8): p. 1587-1594.
14. Wang, Y., et al., *Synthesis and evaluation of [18F]exendin (9-39) as a potential biomarker to measure pancreatic beta-cell mass.* Nucl Med Biol, 2012. **39**(2): p. 167-76.
15. Brom, M., et al., *Non-invasive quantification of the beta cell mass by SPECT with 111In-labelled exendin.* Diabetologia, 2014. **57**(5): p. 950-959.
16. Pattou, F., J. Kerr-Conte, and D. Wild, *GLP-1–Receptor Scanning for Imaging of Human Beta Cells Transplanted in Muscle.* New England Journal of Medicine, 2010. **363**(13): p. 1289-1290.
17. Nyqvist, D., et al., *Donor Islet Endothelial Cells in Pancreatic Islet Revascularization.* Diabetes, 2011. **60**(10): p. 2571.
18. Christoffersson, G., et al., *Clinical and Experimental Pancreatic Islet Transplantation to Striated Muscle: Establishment of a Vascular System Similar to That in Native Islets.* Diabetes, 2010. **59**(10): p. 2569-2578.
19. Svensson, J., et al., *High Vascular Density and Oxygenation of Pancreatic Islets Transplanted in Clusters Into Striated Muscle.* Cell Transplantation, 2011. **20**(5): p. 783-788.
20. Martin, A., M.R. Komada, and D.C. Sane, *Abnormal angiogenesis in diabetes mellitus.* Medicinal Research Reviews, 2003. **23**(2): p. 117-145.
21. Jones, G.L., et al., *Time Course and Quantification of Pancreatic Islet Revasculariztion Following Intraportal Transplantation.* Cell Transplantation, 2007. **16**(5): p. 505-516.

4

Non-invasive in vivo determination of viable islet graft volume by radiolabeled exendin

AUTHORS: ETER W.A., VAN DER KROON I., ANDRALOJC K., BUITINGA M., WILLEKENS S.M.A., FRIELINK C., BOS D., JOOSTEN L., BOERMAN O.C., BROM M. & GOTTHARDT M.

Adapted from: *Scientific Reports* **5**, 15521, doi:10.1038/s41598-017-07815 (2017).

Abstract

Pancreatic islet transplantation is a promising therapy for patients with type 1 diabetes. However, the duration of long-term graft survival is limited due to inflammatory as well as non-inflammatory processes and routine clinical tests are not suitable to monitor islet survival. ^{111}In-exendin-SPECT (single photon emission computed tomography) is a promising method to non-invasively image islets after transplantation and has the potential to help improve the clinical outcome. Whether ^{111}In-exendin-SPECT allows detecting small differences in BCM and precisely measuring the actual volume of islets that were successfully engrafted has yet to be demonstrated. Here, we evaluated the performance of ^{111}In-exendin-SPECT by using an intramuscular islet transplantation model in C3H mice. In vivo imaging of animals transplanted with 50, 100, 200, 400 and 800 islets revealed an excellent linear correlation between SPECT quantification of ^{111}In-exendin uptake and insulin-positive area, demonstrating that ^{111}In-exendin-SPECT accurately measures BCM, whereas SPECT signal originated from islets that were successfully engrafted. The high sensitivity of the method allowed measuring small differences in graft volumes, as well as grafts that contained less than 50 islets. The presented method is reliable, convenient and holds great potential for non-invasive monitoring of BCM after islet transplantation in humans.

Introduction

Transplantation of islets of Langerhans is a promising treatment for patients with type 1 diabetes (T1D). The short-term results of islet transplantation in normalizing blood glucose levels are encouraging [1]. However, the rate of insulin-independency drops to less than 15% after 5 years [2]. Although the loss of transplanted beta cells quickly renders patients insulin-dependent in a life-time perspective, the remaining graft function still exerts a positive effect on glucose homeostasis, reducing late complications and further progression of micro-vascular diseases [3]. Furthermore, the islet grafts lower the amount of insulin required to maintain acceptable blood glucose levels thereby preventing potentially lethal, severe hypoglycemia by improved glycemic control. However, in view of the considerable side effects caused by the immunosuppressive therapy required to prevent graft rejection, improved survival of the transplanted islet is desirable. In order to optimize islet replacement therapy and to prevent loss of graft function, numerous approaches are currently under investigation, including modified immunosuppressive treatments [4-6] and islet encapsulation strategies [7, 8] treatment with growth factors and other hormones, as well as alternative sources for beta cells (i.e. stem cells, tissue bioengineering) [9-14]. In order to monitor the graft volume and optimize new strategies for beta cell replacement a non-invasive technology to visualize viable transplanted islets *in vivo* is warranted. Such a method should be quantitative and sensitive in order to allow the detection of small changes in the number of surviving islets.

A promising approach to visualize transplanted islets *in vivo* has been demonstrated by Saudek et al., using Magnetic Resonance Imaging (MRI). The group described MRI of islets that had been labeled with super-paramagnetic iron oxide particles (SPIOs) prior to transplantation [15]. The feasibility of longitudinal non-invasive monitoring of islet transplants was further demonstrated in animal models by Evgenov and co-workers, successfully monitoring islet transplants for up to 188 days after surgery [16]. Pre-labeling of the islets with SPIOs is therefore a promising method with clinical potential [17].

Alternatively, radionuclide imaging modalities were used because of their high detection sensitivity of transplanted islets. First results of PET imaging of an islet graft were published in 2006, using islets which were transfected with an insulin promoter-dependent reporter gene that leads to trapping of the PET probe ^{18}F-FHBG in islet grafts [18]. In another experiment, islets were pre-labeled with ^{18}F-fluorodeoxyglucose (^{18}F-FDG) and post-transplantation events could be monitored for up to 6 hours after transplantation [19].

More recently, specific targeting of beta cells after *in vivo* injection of radiolabeled exendin followed by SPECT imaging was reported as a promising strategy to non-invasively visualize and quantify BCM in the pancreas of rodents, as well as in healthy and diabetic individuals [20, 21]. Similar exendin-based radiotracers were applied for

non-invasive imaging of islet grafts in rodent transplantation models as well as in human skeletal muscle [22-24]. Although the use of such tracers in a clinical setting of islet transplantation is highly warranted, establishing the correlation between true beta cell mass and the uptake of the radiotracer *in vivo* is an essential validation step before such studies could be conducted in humans. Such decisive step has not been performed for GLP-1R imaging of islet transplants.

In the present study, we measured the uptake of ^{111}In-exendin-3 in transplants consisting of different amounts of islets in the calf muscles of C3H mice by non-invasive SPECT imaging *in vivo* and validated ^{111}In-exendin as a quantitative biomarker for assessment of transplanted beta cell volumes.

Research Design and Methods

Animals. Female C3H/HeNCrl mice (22–30 g) were purchased from Charles River (Calco, Itlay). Experiments were approved by the Animal Ethical Committee of the Radboud University, Nijmegen, The Netherlands.

Pancreatic islet isolation and transplantation. Pancreatic islets were isolated from 6-8 weeks old mice by a collagenase digestion method. Briefly, mice were euthanized and 2 ml of cold RPMI 1640 (Invitrogen, Carmarillo, CA, USA) containing collagenase type V (1 mg/ml; Sigma Aldrich, St Louis, MO, USA) were infused into the pancreatic duct *in situ*. Perfused pancreata were collected in serum-free RPMI medium and kept on ice until enzymatic digestion at 37 °C for 12 min. Islets were purified on a discontinuous Ficoll gradient of following densities: 1.118, 1.096 and 1.037 g/ml (Cellgro by Mediatech Inc., Manassas, VA, USA) and islets were collected between the second and the third fraction. Islets were cultured overnight in a humidified 5 % CO_2 atmosphere at 37 °C in RPMI 1640 medium supplemented with L-glutamine (Sigma Aldrich, St. Louis, MO, USA), penicillin-streptomycin (10 mg/ml; Sigma Aldrich) and 10 % (v/v) fetal calf serum (HyClone, Celbio, Logan, UT, USA). Islets were counted and hand-picked under bright field microscope and 50, 100, 200, 400 or 800 islets were transplanted in the calf muscle, parallel to the fibula, using needles with a 0.8 mm diameter. The exact number of transplanted islets was determined by subtracting the remaining islets in the tube from the initially counted number.

Radiolabeling of exendin-3. [Lys^{40}(DTPA)]-exendin-3 was purchased from Peptide Specialty Laboratories (Heidelberg, Germany). Tracer labeling with In-111 was performed as previously described [20]. Radiochemical purity was determined by ITLC and radiolabeled exendin-3 was purified by solid-phase extraction using a HLB-column as previously reported [20].

SPECT acquisition. Mice with 50, 100, 200, 400 and 800 islets were scanned after 4 weeks. All mice (n=4-5) were injected with approximately 15 MBq of ^{111}In-exendin-3 (peptide dose 0.1 μg in 200 μl PBS, 0.5 % BSA) in the tail vein. SPECT scans were acquired 1 h post-injection on a U-SPECT-II/CT dedicated small-animal scanner (MILabs, Utrecht, Netherlands) for 50 min with a high sensitivity mouse collimator (1.0 mm pinholes). Computed tomography (CT) was performed subsequently for anatomical reference. Standards of 74 kBq, 55 kBq, 37 kBq and 18 kBq in 50 μl volume each, were scanned under the same parameters as reference for quantification. Images were reconstructed with voxel size of 0.4 mm, 3 iterations and 16 subsets, using U-SPECT-II reconstruction software (MILabs, Utrecht, The Netherlands). No attenuation correction was applied. No filtering was performed after reconstruction of the images. The VOI was drawn over the islet transplant region, total voxel intensity registered in the islet graft was corrected by the mean of 3 measurements of contra-lateral control muscle, to subtract the background signal originating from the muscle tissue. The absolute activity (in kBq) was calculated by multiplying the corrected voxel intensity value with the calibration factor determined by quantitative analysis of standards with known radioactivity and data were normalized by the injected dose.

Morphometric analysis of the transplant. Immediately after SPECT acquisitions, mice were euthanized, muscles were fixed in 4% paraformaldehyde and embedded in paraffin, then sectioned into 4 μm slices for autoradiography analysis or for determination of insulin volume by immunohistochemistry. For autoradiography analysis, muscle sections were exposed to an imaging plate (Fuji Film BAS-SE 2025, Raytest, Straubenhardt, Germany) for 7 days and images were visualized with a radioluminography laser imager (Fuji Film BAS 1800 II system, Raytest, Straubenhardt, Germany) and were finally stained with hematoxylin-eosin (HE) to confirm the presence of pancreatic islets. For determination of insulin volume, insulin staining was performed in muscle sections. Antigen retrieval was done using 10 mM sodium citrate buffer, pH 6.0, for 10 min (Thermo Scientific PT module, Lab Vision, USA). Blocking of endogenous peroxidase activity was performed by incubation with 0.6 % H_2O_2 in 40 % methanol / 60 % PBS for 30 min at RT in the dark. An additional blocking step was done with 5 % swine serum in PBS for 30 min at RT. Primary anti-insulin antibody (cat. sc 9168, Santa Cruz Biotechnology, Inc., Santa Cruz, CA, USA) was applied at a dilution of 1:50 (in PBS containing 1 % BSA w/v). Subsequently, sections were washed with PBS and incubated with secondary horseradish peroxidase-conjugated swine-anti-rabbit IgG (1:50) (cat. P0217, Dakopatts, Copenhagen, Denmark) in PBS containing 1 % BSA w/v for 30 min at RT. The staining was visualized with diaminobenzidine (PowerVision™ DAB substrate system, Immunologic, Duiven, The Netherlands) and nuclei were counterstained with haematoxylin. To determine the volume of the transplant, sections were scanned with Pannoramic250 Flash II scanner

(3D Histech, Budapest, Hungary), beta-cell surface was manually drawn around insulin positive region using Photoshop CS6, and the surface was multiplied by the distance separating each analyzed section, which is 40 μm.

Statistical analysis. Correlation studies were expressed as Pearson *r*. Data processing was performed with Graphpad Prism 5 (San Diego CA, USA).

Results

^{111}In-exendin accumulation in the muscle co-localizes with islet transplants. To check whether ^{111}In-exendin-3 signal originates from transplanted islets, C3H mice were transplanted with 800 islets in the calf muscle and were injected with ^{111}In-exendin-3 four weeks after transplantation, where accumulation of the radiotracer in the islets becomes reproducible [25]. Autoradiographical analysis of muscle sections showed tracer accumulation in well localized regions of the tissue (figure 1A) and immunostaining for insulin confirmed that the radioactive signal originated from the islets (figure 1B).

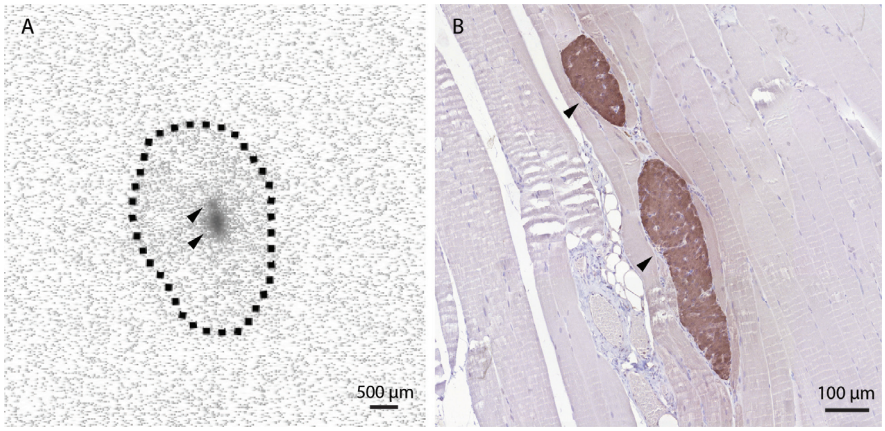

Figure 1 ^{111}In-exendin-3 uptake in the skeletal muscle is co-localized with islet transplants.

(**A**) Autoradiography of muscle sections shows local accumulation of ^{111}In-exendin-3 (black arrows), the limits of the muscle section are shown by the dashed line. (**B**) Immunostaining of the corresponding autoradiography section shows co-localization between beta cells (brown) and ^{111}In-exendin-3.

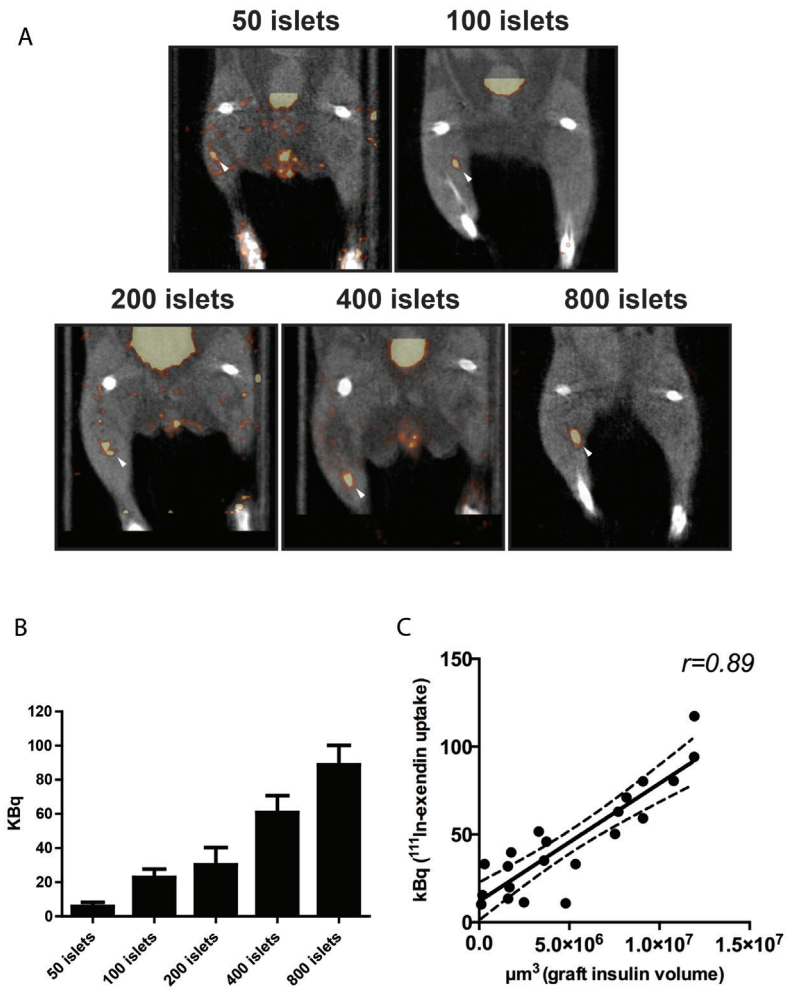

Figure 2 Uptake of ^{111}In-exendin by islet transplants is in linear correlation with transplant size.

(**A**) SPECT imaging detected the grafts initially transplanted with 50, 100, 200, 400 or 800 islets with high sensitivity, 4 weeks after transplantation (white arrows). (**B**) ^{111}In-exendin uptake (expressed in kilobecquerels, kBq) was dependent on transplant size (n=4-5). (C) SPECT signal (expressed in kBq) correlated linearly with graft insulin-positive volume (μm^3) as determined by morphometric analysis of transplant sections (Pearson r=0.89).

^{111}In-exendin uptake by transplanted islets correlates linearly with BCM. ^{111}In-exendin-3 uptake in grafts containing various amounts of islets was detected and clearly delineated by SPECT signal (figure 2A). Quantitative analysis of SPECT signal originating from the transplant revealed differences in ^{111}In-exendin-3 accumulation depending on the number of initially transplanted islets, where the uptake was 5.9 kBq ± 2.4, 22.9 kBq ± 4.8, 30.1 kBq ± 10.1, 60.9 kBq ± 9.8 and 88.7 kBq ± 11.5, in muscles transplanted with 50, 100, 200, 400 and 800 islets, respectively (figure 2B). Immunohistochemical determination of graft volume was performed in all groups of mice (figure 2C). Plotting of SPECT data against the insulin staining volume revealed an excellent linear correlation between ^{111}In-exendin uptake and transplant size (pearson r=0.89).

Discussion

The aim of this study was to measure the uptake of ^{111}In-exendin by islet transplants compared to β-cell mass in a muscle model of islet transplantation. We have demonstrated that tracer uptake and beta-cell volume correlate in an excellent linear manner. In addition, reliable visualization of transplants with various numbers of islets indicates that this method is suitable to quantify small differences in viable β-cells. Tracer uptake was detected in grafts consisting of very low number of islets, demonstrating the high sensitivity of the method.

Previously, imaging of liver islet transplants using ^{64}Cu-labelled exendin has been demonstrated in NOD/SCID mice [22]. Twelve days follow-up of the grafts revealed significantly higher uptake of ^{64}Cu-labeled exendin-4 in the liver of transplanted animals when compared to the control group. Here, we used the skeletal muscle as a highly controlled model for histological verification of insulin positive area, which enabled us to reveal, for the first time, an excellent linear correlation between the numbers of beta cells that were successfully engrafted, and the uptake of the tracer by the grafts.

Recently, it was reported that injection of ^{123}I-IBZM enables the quantification of BCM in islet grafts, where tracer uptake could be linearly correlated with graft volume [26, 27]. However, a far lower correlation was observed between ^{123}I-IBZM uptake and insulin volumes when compared to ^{111}In-exendin, indicating that GLP-1R could allow more accurate assessments of islet graft survival. Exendin displays a much higher uptake in the graft, allowing for detection of lower amounts of transplanted islets. In addition, the higher uptake in the graft as compared to the low background leads to improved quantification as a consequence of the better signal to noise ratio. Finally, our data indicate that ^{111}In-exendin has an advanced detection sensitivity of islet grafts when compared to ^{123}I-IBZM. In fact, more than 50% of the islets could be

lost in the first days after transplantation [28], indicating that ^{111}In-exendin-SPECT could detect grafts containing far less than the 50 islets being initially transplanted. On the other hand, ^{123}I-IBZM-SPECT was able to detect islets in a graft where originally 1000 islets had been transplanted, indicating that grafts containing only low amounts of islets cannot be visualized as with exendin. The superior detection sensitivity of ^{111}In-exendin-SPECT could be explained by the higher abundance of the GLP-1R on the surface of the beta cells when compared to the dopamine 2 receptor [24, 26]. Hence, ^{111}In-exendin-SPECT has the potential to detect small grafts that underwent considerable beta cell loss, and could facilitate treatment assignment or adaptation in order to preserve the remaining islets that could still exert a positive effect on glucose homeostasis.

In summary, ^{111}In-exendin-3 accumulation in islet grafts correlates linearly with living beta cells, and allows the detection of islet grafts consisting of less than 50 islets by SPECT imaging. This indicates that this approach can successfully be applied for accurate and sensitive quantification of viable beta cells.

References

1. Shapiro, A.M.J., et al., *Islet Transplantation in Seven Patients with Type 1 Diabetes Mellitus Using a Glucocorticoid-Free Immunosuppressive Regimen.* New England Journal of Medicine, 2000. **343**(4): p. 230-238.
2. Ryan, E.A., et al., *Five-Year Follow-Up After Clinical Islet Transplantation.* Diabetes, 2005. **54**(7): p. 2060-2069.
3. Thompson, D.M., et al., *Reduced Progression of Diabetic Microvascular Complications With Islet Cell Transplantation Compared With Intensive Medical Therapy.* Transplantation, 2011. **91**(3): p. 373-378.
4. Fandrich, F. and H. Ungefroren, *Customized cell-based treatment options to combat autoimmunity and restore beta-cell function in type 1 diabetes mellitus: current protocols and future perspectives.* Adv Exp Med Biol, 2010. **654**: p. 641-65.
5. Cozzi, E., *On the road to clinical xenotransplantation.* Transpl Immunol, 2009. **21**(2): p. 57-9.
6. Cozzi, E. and E. Bosio, *Islet xenotransplantation: current status of preclinical studies in the pig-to-nonhuman primate model.* Curr Opin Organ Transplant, 2008. **13**(2): p. 155-8.
7. Lee, B.R., et al., *In situ formation and collagen-alginate composite encapsulation of pancreatic islet spheroids.* Biomaterials, 2012. **33**(3): p. 837-45.
8. Basta, G., et al., *Long-term metabolic and immunological follow-up of nonimmunosuppressed patients with type 1 diabetes treated with microencapsulated islet allografts: four cases.* Diabetes Care, 2011. **34**(11): p. 2406-9.
9. Guney, M.A., et al., *Connective tissue growth factor acts within both endothelial cells and beta cells to promote proliferation of developing beta cells.* Proc Natl Acad Sci U S A, 2011. **108**(37): p. 15242-7.
10. Courtney, M., et al., *In vivo conversion of adult alpha-cells into beta-like cells: a new research avenue in the context of type 1 diabetes.* Diabetes Obes Metab, 2011. **13 Suppl 1**: p. 47-52.
11. Brolen, G.K., et al., *Signals from the embryonic mouse pancreas induce differentiation of human embryonic stem cells into insulin-producing beta-cell-like cells.* Diabetes, 2005. **54**(10): p. 2867-74.
12. Sordi, V. and L. Piemonti, *Mesenchymal stem cells as feeder cells for pancreatic islet transplants.* Rev Diabet Stud. **7**(2): p. 132-43.
13. Sordi, V., et al., *Mesenchymal cells appearing in pancreatic tissue culture are bone marrow-derived stem cells with the capacity to improve transplanted islet function.* Stem Cells. **28**(1): p. 140-51.
14. D'Amour, K.A., et al., *Production of pancreatic hormone-expressing endocrine cells from human embryonic stem cells.* Nat Biotechnol, 2006. **24**(11): p. 1392-401.
15. Jirak, D., et al., *MRI of transplanted pancreatic islets.* Magn Reson Med, 2004. **52**(6): p. 1228-33.
16. Evgenov, N.V., et al., *In vivo imaging of islet transplantation.* Nat Med, 2006. **12**(1): p. 144-8.
17. Saudek, F., et al., *Magnetic Resonance Imaging of Pancreatic Islets Transplanted Into the Liver in Humans.* Transplantation, 2010. **90**(12): p. 1602-1606.
18. Lu, Y., et al., *Noninvasive imaging of islet grafts using positron-emission tomography.* Proc Natl Acad Sci U S A, 2006. **103**(30): p. 11294-9.
19. Toso, C., et al., *Positron-emission tomography imaging of early events after transplantation of islets of Langerhans.* Transplantation, 2005. **79**(3): p. 353-5.
20. Brom, M., et al., *Non-invasive quantification of the beta cell mass by SPECT with 111In-labelled exendin.* Diabetologia, 2014. **57**(5): p. 950-959.
21. Brom, M., et al., *111In-exendin uptake in the pancreas correlates with the beta cell mass and not with the alpha cell mass.* Diabetes, 2014.
22. Wu, Z., et al., *Development and Evaluation of 18F-TTCO-Cys40-Exendin-4: A PET Probe for Imaging Transplanted Islets.* Journal of Nuclear Medicine, 2013. **54**(2): p. 244-251.
23. Pattou, F., J. Kerr-Conte, and D. Wild, *GLP-1–Receptor Scanning for Imaging of Human Beta Cells Transplanted in Muscle.* New England Journal of Medicine, 2010. **363**(13): p. 1289-1290.
24. van der Kroon, I., et al., *Noninvasive imaging of islet transplants with 111In-exendin-3.* Journal of Nuclear Medicine, 2016.
25. Eter, W.A., et al., *Graft revascularization is essential for non-invasive monitoring of transplanted islets with radiolabeled exendin.* Scientific Reports, 2015. **5**: p. 15521.

26. Willekens, S., et al., *Quantitative imaging of transplanted pancreatic islets with SPECT using I-123 labeled benzamide.* Journal of Nuclear Medicine, 2015. **56**(supplement 3): p. 592.
27. Willekens, S.M.A., et al., *SPECT of Transplanted Islets of Langerhans by Dopamine 2 Receptor Targeting in a Rat Model.* Molecular Pharmaceutics, 2016. **13**(1): p. 85-91.
28. Biarnés, M., et al., β-Cell Death and Mass in Syngeneically Transplanted Islets Exposed to Short- and Long-Term Hyperglycemia. Diabetes, 2002. **51**(1): p. 66-72.

5

Effect of hyperglycemia on in vivo quantification of beta cell mass with radiolabeled exendin

AUTHORS: ETER W.A., BUITINGA M., FRIELINK C., BROM M. & GOTTHARDT M.

Manuscript under preparation

Introduction

Islet transplantation is a promising experimental approach to reverse hyperglycemia in type 1 diabetic individuals [1]. However, a number of stress factors such as gluco/lipo-toxicity, specific immune-assaults and instant blood-mediated inflammatory reaction (IBMIR) lead to decline in graft function and survival [2-5]. Current clinical tests cannot determine whether graft failure and relapse into hyperglycemia is caused by β-cell dysfunction or death [6, 7]. Non-invasive tools are, therefore, warranted to determine BCM after transplantation, independently of graft function. Molecular imaging has emerged as a promising tool to quantify BCM after specific targeting of β-cell surface markers. The glucagon-like peptide-1 receptor (GLP-1R) is an attractive biomarker which is specifically expressed on the β-cell surface and not in α, δ and pp cells [8]. *In vivo* targeting of the GLP1-R using ^{111}In-exendin, followed by SPECT (Single Photon Emission Computed Tomography) was demonstrated as a promising strategy to visualize and quantify small differences in BCM in the pancreas of healthy and diabetic individuals [9]. In addition, the GLP-1R can also be used as a target for BCM assessment in engrafted islets [10].

Islet transplantation is performed in subjects with long-standing history of brittle diabetes and with frequent episodes of hypoglycemia. Long-term exposure of β-cells to hyperglycemia has a detrimental effect on their survival, replicative and functional capacities [3, 11, 12]. In addition, it was reported that GLP-1R expression is down-regulated both *in vitro* and *in vivo* after long-term exposure of the β-cells to hyperglycemia [13-15]. Finally, the therapeutic effect of incretin-based pharmaceuticals on type 2 diabetes patients (e.g. with the GLP-1 analogue, exenatide) is hampered by elevated blood glucose levels [16], while being more effective in patients with well-regulated blood glucose levels [17]. These clinical observations could be explained by, for instance, downregulation of the GLP-1R expression by the β-cells [13]. Hence, the effect of hyperglycemic stress on ^{111}In-exendin uptake by the β-cells for BCM quantification should be assessed for determination of optimal protocols for *in vivo* imaging of BCM by this method.

The aims of this study were to determine the effects of sustained hyperglycemia on ^{111}In-exendin accumulation in islets transplanted in the skeletal muscle of diabetic (alloxan-treated) mice and to determine if GLP-1R is a reliable biomarker to quantify living β-cells during hyperglycemia and after establishing glycemic control.

Research Design and Methods

Animals. Female C3H/HeNCrl mice (22–30 g) were purchased from Charles River (Calco, Itlay). All experiments were conducted in accordance with Radboud Univserity guidelines and on humane care and use of laboratory animals.

Experimental groups. Mice were injected i.v. with 75 mg/kg of alloxan (Sigma, St Louis, MO, USA) as previously described [9]. Experiments started after hyperglycemia was confirmed (25-30mmol/L) by using a glucose meter (Accu-Chek Sensor; Roche Diagnostics; Almere, The Netherlands).

Mice assigned to the control group (group 1) received subcutaneous injection of insulin implants (LinShin, Toronto, Ontario, Canada) 7 days after alloxan injection (5-9 mmol/L) and were transplanted with islets after 14 days, where glycemic levels were stabilized for at least 5 days. SPECT imaging was performed 4 weeks after transplantation. Mice assigned to the discontinued insulin-treatment group (group 2) were treated with insulin 7 days after alloxan injection, for a period of 14 days (5-9 mmol/L) prior to islet transplantation, and insulin pellets were surgically removed 14 days after transplantation to re-induce hyperglycemia (5-9mmol/L then 24-30 mmol/L). SPECT imaging was performed after 4 weeks of hyperglycemia. Mice assigned to the insulin-treated group (group 3) were treated with insulin 7 days after alloxan injection, for a period of 14 days (5-9 mmol/L) prior to islet transplantation, and insulin pellets were surgically removed 14 days after transplantation to re-induce hyperglycemia (24-30 mmol/L). Finally, mice were re-treated with insulin pellets to re-establish normoglycemia (5-9mmol/L). SPECT imaging was performed after 2 weeks of normoglycemia.

Islet isolation and transplantation. Pancreatic islets were isolated from 8 weeks-old female C3H/HeNCrl donor mice by collagenase digestion method and recipients were transplanted with 200 islets in the calf muscle as previously described [10]. Number of transplanted islets was determined as insufficient to reverse hyperglycemia.

Radiolabeling. [Lys^{40}(DTPA)]-exendin-3 was purchased from Peptide Specialty Laboratories (Heidelberg, Germany). Radiolabeling procedure was performed as previously described [9]. Radiochemical purity was evaluated by ITLC and the radiolabel was purified by solid-phase extraction using a HLB-cartridge (Waters, Etten-Leur, The Netherlands) before animal injection [9]. Animals were injected with 0.1 μg of exendin-3 radiolabeled with approximately 15 MBq in a 0.5% bovine serum albumin solution in 200 μl phosphate-buffered saline.

Imaging procedure and data acquisition. All mice were scanned 1 hour post injection of ^{111}In-exendin. Scans were performed with a small animal U-SPECT-II/CT system (MILabs, Utrecht, The Netherlands) using a 1 mm multi-pinhole ultra-high sensitivity mouse collimator for 50 minutes. Groups 1 and 2 were scanned 4 weeks after transplantation and group 3 was scanned 6 weeks after transplantation. CT scans were performed in full/accurate mode under 615 μA/s and 65 kV. After SPECT/CT acquisitions, animals were euthanized and calf muscles containing the transplant were extracted and incubated in 1% paraformaldehyde inside eppendorf tubes where *ex vivo* scans were acquired for 12 hours. SPECT data were reconstructed using OSEM (3 iterations, 16 subsets, voxel size 0.4 mm) with the U-SPECT-Rec software (MILabs, Utrecht, The Netherlands). To quantify SPECT signal, a volume of interest (VOI) was drawn in the area of the transplant and the background was subtracted after applying similar VOI on contra-lateral calf muscle that did not contain islets. Data were corrected for the injected dose and converted to kBq by using standards with known activity scanned and reconstructed under similar settings.

Immunohistochemistry. For autoradiography, muscles containing the transplant were embedded in paraffin and 4 μm thick sections were cut at separate levels of the tissue with 40 μm distance. Muscle sections were exposed to an imaging plate (Fuji Film BAS-SE 2025, Raytest, Straubenhardt, Germany) for one week. Images were visualized with a radioluminography laser imager (Fuji Film BAS 1800 II system, Raytest, Straubenhardt, Germany). Quantification of the autoradiographical images was performed with AIDA Image Analyzer software (Raytest GmbH, Straubenstadt, Germany). Radioactivity accumulation in the transplants was measured by drawing ROIs around each transplant as well as around the standards with known amount of radioactivity. For measurement of insulin area in the autoradiography corresponding transplants, sections were processed for antigen retrieval by incubating in 10 mM citrate pH 6 for 10 min at 96 °C and blocked with 1% BSA (w/v in PBS) for 30 min and endogenous peroxidase activity was blocked with 3% H_2O_2 (v/v in PBS) for 30 min. Staining was performed with anti-insulin rabbit antibody (Santa Cruz Biotechnology, Santa Cruz, CA, USA) diluted 1/50 during 1 hour at room temperature. Sections were next incubated with swine anti-rabbit conjugated with peroxidase, during 30 min at room temperature and washed with PBS. Finally, hematoxylin counterstaining was performed and sections were visualized by bright field microscopy (Leica Microsystems, Wetzlar, Germany). Autoradiography data was normalized by the insulin area measured in the corresponding section and was expressed in Bq (Becquerel).

Results

Islet transplants can be detected with ^{111}In-exendin-3 and SPECT during hyperglycemia and after restoring normoglycemia. To determine whether islet transplants can be detected during severe hyperglycemia and after insulin treatment, group 1 (control), group 2 (discontinued insulin-treatment) and group 3 (insulin-treated) were injected with ^{111}In-exendin and were scanned under the same parameters. Islets were detected in all groups of mice (figure 1 A-C). SPECT signal was lower in recipients that were scanned after prolonged periods of hyperglycemia. On the other hand, SPECT signal was higher after insulin treatment.

Blood glucose levels influence ^{111}In-exendin-3 accumulation in islet transplants. In order to determine the effect of blood glucose levels on ^{111}In-exendin-3 accumulation in islet transplants, we performed *ex vivo* autoradiography on muscle sections containing the islets, followed by insulin staining (figure 2A-C). There was accumulation of ^{111}In-exendin-3 within well-localized regions of the muscle in all groups of mice, which was in co-localization with insulin staining.

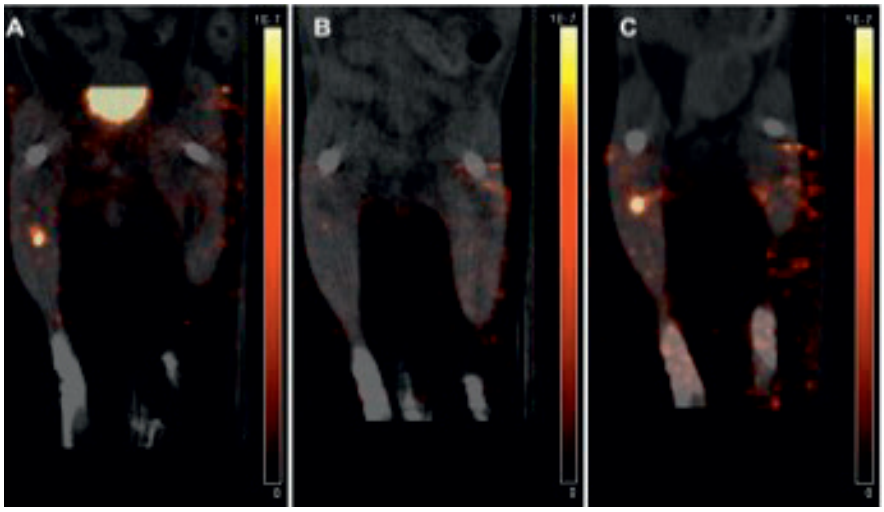

Figure 1 SPECT imaging of islet transplants with ^{111}In-exendin.

(**A**) SPECT imaging detected islet grafts in group 1. (**B**) SPECT signal was decreased after four weeks of hyperglycemia (group 2). (**C**) Tracer uptake has recovered after insulin treatment (group 3).

Quantification of tracer accumulation in islet grafts revealed lower tracer uptake per insulin area after a severe and prolonged period of hyperglycemia, when compared to the control group (figure 2D). Importantly, after 2 weeks of continuous insulin treatment, tracer uptake was restored and became comparable to the control group. Linear correlation between insulin area and exendin-3 uptake was observed for all groups of mice.

Similarly, tracer uptake in the pancreas of the recipients was significantly decreased by elevated blood glucose levels and was restored after insulin treatment (figure 3).

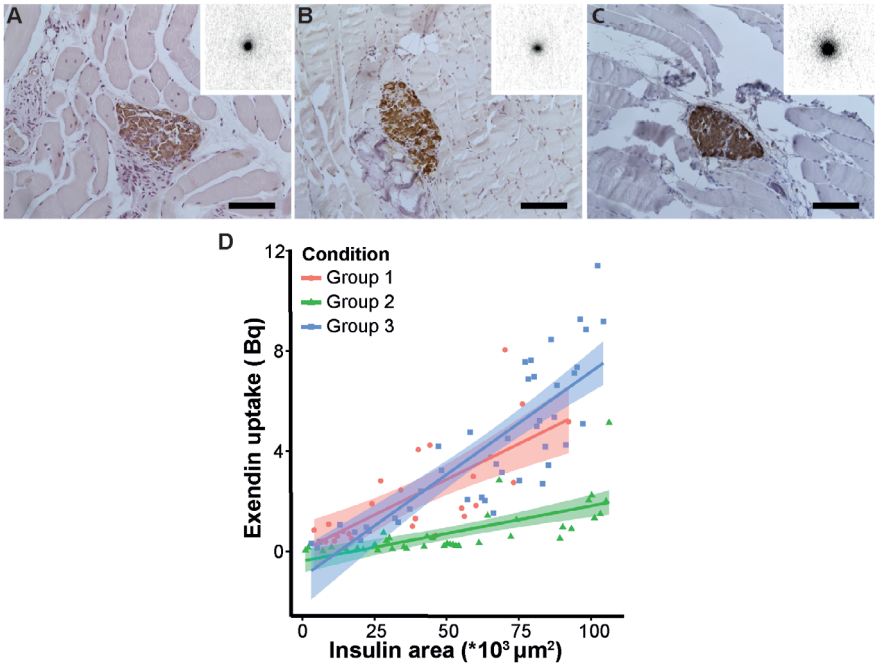

Figure 2 ^{111}In-exendin uptake by islet grafts is affected by blood glucose levels.

Autoradiography analysis and insulin staining showed co-localization between exendin uptake and β-cells, in (A) group 1, (B) group 2 and (C) group 3. (D) Quantitative analysis of autoradiography revealed linear correlation between tracer uptake and insulin areas in all groups of mice, while tracer uptake per insulin area was decreased in group 2 when compared to group 1 and 3. Colored area around the linear regression represent the confidence intervals ($p<0.95$).

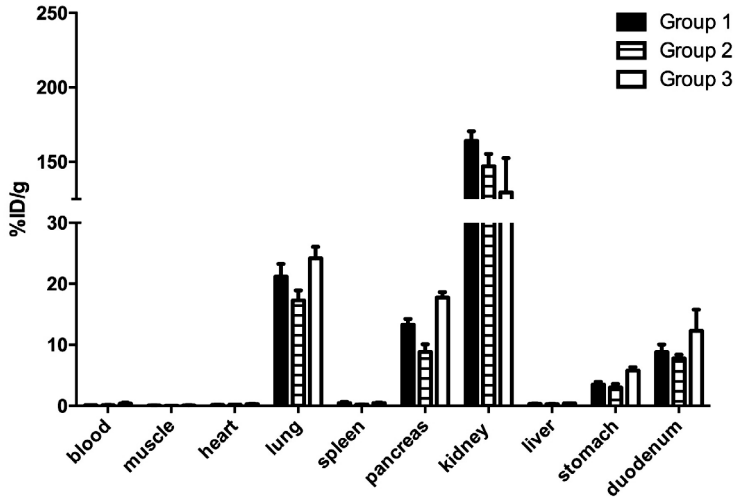

Figure 3 Biodistribution of ^{111}In-exendin in control, hyperglycemic and insulin-treated groups.

^{111}In-exendin uptake was observed in organs known to express the GLP-1R in all groups of mice. Tracer accumulation was decreased during hyperglycemia, and increased after insulin treatment in the exendin-targeted organs.

Discussion

In the present study, we examined the effect of glycemia on the uptake of ^{111}In-exendin-3 by islet transplants. We demonstrated that increased blood glucose levels 2 weeks after transplantation results in decreased accumulation of ^{111}In-exendin-3 in the transplant. Restoring of blood glucose control for a period of 2 weeks, subsequent to 4 weeks of hyperglycemia, restores the level of tracer uptake by the islets. These results indicate that blood glucose levels have a direct influence on BCM quantification and must be considered when measuring islet graft survival. Imaging of islet transplants with radiolabeled exendin will reveal reliable results when normoglycemia is achieved 2 weeks prior to targeting of the islets with radiolabeled exendin.

Detection of islet grafts with SPECT was feasible during normoglycemia, as well as hyperglycemia. Autoradiography-based analysis of islet sections revealed that changes in SPECT signal were not due to changes in BCM, given the differences in tracer uptake per insulin-positive area. Decreased tracer accumulation in the islets during hyperglycemia is in accordance with clinical observations, where type 2 diabetes patients exhibit an impaired response to incretin-based treatments [13, 16].

Several processes could explain the decrease in exendin-3 uptake by the beta cells during hyperglycemia. One possibility is down-regulation of GLP-1R expression by the beta cells. Another possibility is, that exendin-3 internalization after binding to GLP-1R is hampered due to changes in the downstream signaling systems [14], causing less efficient trapping of the tracer inside the beta cells [18]. Finally, the effect of prolonged hyperglycemia on decreasing intra-islet blood flow could result in impaired delivery of the radiotracer to the islets [19]. Restoration of tracer uptake by the islets after achieving normoglycemia indicates that the mechanisms involved in this process are reversible. This is in accordance with clinical observations, where type 2 diabetes patients with well-regulated blood glucose levels have an effective response to incretin actions [13, 16, 17].

In line with previous study [20], tracer uptake allowed to determine the BCM in healthy islet recipients. We also observed a linear correlation between BCM and tracer uptake during hyperglycemia, despite the decreased uptake per insulin area. As we do not know whether there is a threshold for hyperglycemia to cause reduction of exendin uptake, we believe that exendin scans should be performed under euglycemic conditions or at least, under comparable glycemic conditions, the latter potentially leading to higher patient numbers required for inter-individual comparison in clinical studies.

It was demonstrated that exendin-3 uptake in the pancreas allows to detect small differences in the BCM between healthy and diabetic subjects [9]. Here, uptake in the pancreas (as well as in islet transplants) was decreased by hyperglycemia, as compared to the insulin-treated group, and was restored after 2 weeks of normoglycemia. We therefore suggest that normoglycemia should be achieved prior to BCM quantification with ^{111}In-exendin.

In conclusion, this study reveals that blood glucose level is a key physiological parameter to consider when quantifying BCM by *in vivo* targeting of the GLP-1R with ^{111}In-exendin-3. Reliable quantification of BCM using exendin-3 can be achieved 2 weeks after restoring normoglycemia, where tracer uptake is no longer affected by beta cell hyperglycemic stress.

References

1. Shapiro, A.M.J., et al., *Islet Transplantation in Seven Patients with Type 1 Diabetes Mellitus Using a Glucocorticoid-Free Immunosuppressive Regimen.* New England Journal of Medicine, 2000. **343**(4): p. 230-238.
2. Lee, Y., et al., *Metabolic Mechanisms of Failure of Intraportally Transplanted Pancreatic β-Cells in Rats: Role of Lipotoxicity and Prevention by Leptin.* Diabetes, 2007. **56**(9): p. 2295-2301.
3. Biarnés, M., et al., β-Cell Death and Mass in Syngeneically Transplanted Islets Exposed to Short- and Long-Term Hyperglycemia. Diabetes, 2002. **51**(1): p. 66-72.
4. Nilsson, B., K.N. Ekdahl, and O. Korsgren, *Control of instant blood-mediated inflammatory reaction to improve islets of Langerhans engraftment.* Current Opinion in Organ Transplantation, 2011. **16**(6): p. 620-626.
5. Ryan, E.A., et al., *Five-Year Follow-Up After Clinical Islet Transplantation.* Diabetes, 2005. **54**(7): p. 2060-2069.
6. Roep, B.O., et al., *Auto- and alloimmune reactivity to human islet allografts transplanted into type 1 diabetic patients.* Diabetes, 1999. **48**(3): p. 484-490.
7. Pileggi, A., et al., *Factors influencing Islet of Langerhans graft function and monitoring.* Clinica Chimica Acta, 2001. **310**(1): p. 3-16.
8. Tornehave, D., et al., *Expression of the GLP-1 Receptor in Mouse, Rat, and Human Pancreas.* Journal of Histochemistry & Cytochemistry, 2008. **56**(9): p. 841-851.
9. Brom, M., et al., *Non-invasive quantification of the beta cell mass by SPECT with 111In-labelled exendin.* Diabetologia, 2014. **57**(5): p. 950-959.
10. Eter, W.A., et al., *Graft revascularization is essential for non-invasive monitoring of transplanted islets with radiolabeled exendin.* Scientific Reports, 2015. **5**: p. 15521.
11. Monta, et al., *Beta cell mass and growth after syngeneic islet cell transplantation in normal and streptozocin diabetic C57BL/6 mice.* The Journal of Clinical Investigation, 1993. **91**(3): p. 780-787.
12. Nacher, V., et al., *Normoglycemia Restores β-Cell Replicative Response to Glucose in Transplanted Islets Exposed to Chronic Hyperglycemia.* Diabetes, 1998. **47**(2): p. 192-196.
13. Xu, G., et al., *Downregulation of GLP-1 and GIP Receptor Expression by Hyperglycemia: Possible Contribution to Impaired Incretin Effects in Diabetes.* Diabetes, 2007. **56**(6): p. 1551-1558.
14. Rajan, S., et al., *Chronic hyperglycemia downregulates GLP-1 receptor signaling in pancreatic β-cells via protein kinase A.* Molecular Metabolism, 2015. **4**(4): p. 265-276.
15. Kim, D.-I., et al., *Hyperglycemia-induced GLP-1R downregulation causes RPE cell apoptosis.* The International Journal of Biochemistry & Cell Biology, 2015. **59**: p. 41-51.
16. Holst, J.J., et al., *Loss of Incretin Effect Is a Specific, Important, and Early Characteristic of Type 2 Diabetes.* Diabetes Care, 2011. **34**(Supplement 2): p. S251.
17. An, Z., R.L. Prigeon, and D.A. D'Alessio, *Improved Glycemic Control Enhances the Incretin Effect in Patients With Type 2 Diabetes.* The Journal of Clinical Endocrinology & Metabolism, 2013. **98**(12): p. 4702-4708.
18. Brom, M., et al., *Radiolabelled GLP-1 analogues for in vivo targeting of insulinomas.* Contrast media & molecular imaging, 2012. **7**(2): p. 160-166.
19. Jansson, L. and S. Sandler, *Influence of Hyperglycemia on Blood Perfusion of Autotransplanted Pancreatic Islets in Diabetic Rats.* Diabetes, 1989. **38**(Supplement 1): p. 196-198.
20. van der Kroon, I., et al., *Noninvasive Imaging of Islet Transplants with 111In-Exendin-3 SPECT/CT.* J Nucl Med, 2016. **57**(5): p. 799-804.

6

SPECT-OPT multimodal imaging enables accurate evaluation of radiotracers for beta-cell mass assessments

AUTHORS: ETER W.A. [1], PARWEEN S. [2], JOOSTEN L. [1], FRIELINK C. [1], ERIKSSON M. [2], BROM M. [1], AHLGREN U. [2] & GOTTHARDT M. [1]

[1] Department of Radiology and Nuclear Medicine, Radboud University Medical Center, Nijmegen, The Netherlands.

[2] Umeå Centre for Molecular Medicine, Umeå University, Umeå, Sweden.

Adapted from: *Scientific Reports* **6**, 24576, doi: 10.1038/srep24576 (2016).

Abstract

In-vivo targeting of the GLP1-R with ^{111}In-exendin-3 followed by Single Photon Emission Computed Tomography (SPECT) has become a promising experimental approach to monitor changes in β-cell mass (BCM) during diabetes progression. SPECT imaging of pancreatic islets is most commonly cross-validated by stereological analysis of histological pancreatic slices subsequent to insulin staining. Typically, stereological methods do not accurately determine the total β-cell volume, which is inconvenient when correlating total pancreatic tracer uptake with BCM. Alternative methods are therefore warranted to cross-validate β-cell imaging using radiotracers. Here, we evaluated optical projection tomography (OPT), a technique that provides 3-D quantitative imaging of the pancreatic islets, for cross-validating radionuclide-based imaging of β-cells. Uptake of ^{111}In-exendin-3 was measured by SPECT and was correlated with histology as well as OPT-based quantification of insulin positive areas within healthy and alloxan-treated Brown Norway rat pancreata. SPECT signal was in excellent linear correlation with OPT data as compared to histology. While histological determination of islet spatial distribution was challenging, SPECT and OPT revealed similar distribution patterns of ^{111}In-exendin and β-cell distribution across the pancreas. Here, we introduce SPECT-OPT multimodal imaging as highly accurate strategy for validating the performance of β-cell radiotracers.

Introduction

The prevalence of diabetes is 415 million worldwide and the numbers are on the rise [1]. Both β-cell dysfunction and death contribute to diabetes progression. The relationship between β-cell mass (BCM) and function is not clear and therefore, the routine immunological and functional tests are not suitable to monitor changes in BCM [2-4] . There is a high interest in developing non-invasive tools to quantify BCM, independently of their function, to better understand the progress of the disease. Current non-invasive imaging techniques, with the highest anatomic resolution available, are not powerful enough to detect single islets *in vivo* and in humans at this point in time. Alternatively, radioactive-based imaging methods are used for their advanced detection sensitivity of tracer uptake by β-cells [5, 6]. Specific targeting of β-cells by ^{111}In-exendin-3 followed by SPECT was reported as a promising tool to detect and quantify small differences in BCM in T1D rodent models as well as T1D patients [7]. These findings were validated by the linear correlation between ^{111}In-exendin uptake and histological quantitative analysis of BCM in rodents. Although comparison between radioactive imaging and two-dimensional stereological techniques is a conventional research practice, which benefits from the possibility to correlate tracer uptake with the quantification of insulin producing β-cells at (sub-)cellular resolution, such a method is associated with several disadvantages. Typically, stereological techniques rely on certain assumptions, in particular regarding the degree of convexity of the islets and their orientation/distribution within the gland, to estimate islet β-cell volume or mass. In addition, such techniques are highly labor and time consuming and are, consequently, performed by interval or random sampling, even for limited cohorts of animals. Therefore, the outcome will inevitably be an extrapolation of two-dimensional information. It has been demonstrated that the islet β-cells are differing in size and are heterogeneously distributed within the organ, both with respect to the individual lobular compartments and between the lobes [8, 9]. In addition, different regions of the pancreas could be unequally affected by diabetes in different animals of the same strain and stage [10], further complicating the picture. Hence, sampling techniques are, depending on the analyzed model, prone to over- or underestimate the true BCM, and are largely dependent on the chosen quantification method. Indeed, the establishment of a stereological approach to describe the complete pancreatic islet-volume distribution has been described as a “true stereological challenge” [11]. Consequently, an alternative strategy to correlate radiotracer uptake in the pancreas with actual BCM is needed.

Previous studies developed an OPT-based method that allows visualizing and studying fixated biological specimens at high spatial resolution [12]. This technique was shown remarkably accurate for quantifying BCM and determining the spatial distribution within and between the lobes of the pancreas down to the resolution of

single islets after ex-vivo antibody-based targeting of insulin [8, 9, 13]. Importantly, OPT allows to scan a sample with high resolution on the millimeter to centimeter-scale [14], thereby being a technique of choice to image complete lobes of murine pancreas [8, 13].

Here, we sought to determine whether fast and accurate cross-validation of radionuclide-based imaging of β-cells can be achieved by sequential SPECT-OPT multimodal imaging, as compared to SPECT followed by histology. Uptake of ^{111}In labeled [Lys^{40}(DTPA)$_6$]-exendin-3 by the β-cells was quantified by SPECT and was cross-examined by histology and OPT-based assessment of insulin volume in the splenic, gastric and duodenal lobes [14] of healthy and alloxan-treated diabetic of Brown Norway (BN) rats.

Research Design and Methods

Animals and alloxan treatment. Female Brown Norway rats (110-120 g) were purchased from Charles River (Calco, Itlay). All experiments were conducted in accordance with Radboud Univserity and Umeå University guidelines on use of laboratory animals. Experiments were approved by the Animal Ethical Committee of the Radboud University, Nijmegen, The Netherlands and the Ethical Committee for Animal Research, Northern Sweden. Rats assigned to the diabetic group were injected intravenously with 60 mg/kg of alloxan (Sigma, St Louis, MO, USA) as previously described [7] and animals assigned to the healthy group were injected with the vehicle compound. Experiments started after confirmation of hyperglycemia (>20mmol/L) in alloxan-treated rats by using a glucose meter (Accu-Chek Sensor; Roche Diagnostics; Almere, The Netherlands), namely 7 days after the injection.

Radiolabeling of exendin-3. [Lys^{40}(DTPA)$_6$]-exendin-3 was purchased from Peptide Specialty Laboratories (Heidelberg, Germany). Peptide labeling with In-111 and quality controls were performed as previously described [7]. All animals were injected with 20pmol of exendin-3 corresponding to approximately 150 MBq.

SPECT imaging and data acquisition. Rats were intravenously injected with radio-labeled exendin-3 and euthanized 1 hour post-injection. The pancreata were isolated and the splenic, gastric and duodenal lobes were separated. Finally, lobes were fixed in 4% PFA for two hours and were scanned in phosphate buffered saline (PBS) with the small animal U-SPECT-II/CT system (MILabs, Utrecht, The Netherlands) with a 0.2 mm multi-pinhole collimator for 12 hours. Images were reconstructed with OSEM (3 iterations, 16 subsets, voxel size 2 mm) using the U-SPECT-Rec software (MILabs, Utrecht, The Netherlands) and the measured counts were converted to kBq (Kilobecquerels) using standards with known radioactivity concentrations scanned

with the same settings. After SPECT acquisitions, lobes were measured for radioactivity in a γ-counter (Wallac 1480 Wizard, Perkin Elmer, Boston, MA, USA) and data were expressed as the percentage of administered dose.

OPT imaging and data acquisition. After quantification of radioactivity, pancreata were stepwise dehydrated in 33%, 66% and 100 % methanol and stored at -20°C. Tissue samples were next stained for Insulin (Primary antibody Guinea Pig anti-insulin, (DAKO: A0564) and secondary antibody IRDye 680 anti-Guinea Pig (Licor: 926-68077)) and processed for OPT imaging essentially as described previously [13]. OPT scans were performed for individual lobes using a Near Infrared-OPT (NIR-OPT) setup with excitation filter 665/45 and emission filter 725/50 as described previously [13]. The anatomy of the pancreas, based on its auto-fluorescence, was obtained by scanning it with a excitation 480/40 and emission 510LP filter set. Tomographic reconstruction was performed essentially as described [13]. Contrast limited adaptive histogram equalization (CLAHE) was not needed due to a good signal to noise ratio obtained in volume rendering data. Insulin stained β cell volume was quantified by generating 3D iso-surface based on signals from individual islets using Imaris 7.7. software (Bitplane).

Immunohistochemistry and morphometric analysis. Following OPT scans, the specimens were treated with methanol 4-5 times (for 3-4 days) and were rehydrated with 70%, 50%, 30% and 10% ethanol. Excess of agarose was trimmed off when the samples were in 10% ethanol and then incubated in 0.29 M sucrose for 60 min at room temperature followed by incubation in preheated 0.29 M sucrose at 57 °C to completely remove residual agarose and washed in PBS. Next, the pancreata were subjected to paraffin embedding and 4 μm thick sections were produced at 3 separate levels of the tissue with 100 μm distance. Sections were submitted for antigen retrieval during 10 min in 10 mM citrate pH 6 at 96°C and blocked with 1% BSA in PBS for 30 minutes and endogenous peroxidase activity was blocked with 3% H_2O_2 in PBS for 30 minutes. Staining was performed using anti-insulin rabbit antibody (Santa Cruz Biotechnology, Santa Cruz, CA, USA) diluted 1/50 for 1 hour at room temperature and washed in PBS. Sections were next incubated with swine anti-rabbit conjugated with peroxidase, for 30 min at room temperature and washed with PBS. Finally, hematoxylin counterstaining was performed and sections were scanned with Pannoramic250 Flash II scanner (Budapest, Hungary). BCM was next estimated by measuring the average of insulin staining areas of 3 sections per lobe (expressed in μm^2) separated by 100 μm. The quantification was performed using Adobe Photoshop CS5 Version 12.0.

Statistical analysis. Values are expressed as means ± SEM. Student t-test was performed for comparisons, where P value <0.05 was considered as statistically significant. To assess whether the correlation of SPECT-OPT and SPECT-histology differs, comparisons were performed using multiple linear regression analysis (ANCOVA). All statistical tests were performed with Graphpad Prism 5 (GraphPad Software, San Diego California USA).

Results

Correlation of SPECT imaging with morphometric determination of BCM. ^{111}In-exendin-3 uptake was quantified by SPECT imaging of single pancreatic lobes from healthy and diabetic animals, and the accuracy of the measurements was verified by the linear correlation between SPECT data and gamma-counter based analysis of radioactivity (r^2=0.85) (Supplementary Figure S1 A). Healthy rats showed higher accumulation of radioactivity (measured by gamma-counter) per gram of pancreatic tissue when compared to the diabetic group (Supplementary Figure S2 A).

Morphometric analysis of insulin staining was conducted at three different levels of each pancreatic lobe (Figure 1A-B). Insulin stained BCM (mg) in alloxan treated pancreata was significantly reduced to 7.94% in comparison with the healthy group ($p<0.001$) (Figure 1C). Spatial quantitative analysis of β-cells did not show any significant differences in their distribution between the pancreatic lobes (Figure 1D). In line with our previous studies [7], we observed a linear correlation between ^{111}In-exendin-3 uptake and insulin positive area per lobe (r^2= 0.52) (Figure 1E). Similarly, a linear correlation was observed between SPECT and histological based analysis of total BCM (r^2=0.53) (Supplementary Figure S1 B).

Multimodal imaging of rat pancreatic lobes with SPECT and OPT. High uptake of ^{111}In-exendin-3 was observed by SPECT in the pancreas of healthy rats (Figure 2A). This was in line with the abundant insulin staining visualized by OPT (Figure 2C). Rats that were treated with alloxan prior to SPECT and OPT imaging exhibited decreased signal by both modalities (Figure 2B and D). Furthermore, the distribution of ^{111}In-exendin-3 accumulation was similar to the distribution of the β-cells observed by OPT. Quantification of ^{111}In-exendin-3 uptake showed an accumulation of 55.46 ± 5.55 kBq in the pancreas and a total β-cell volume of $1.18\text{x}10^{10}$ ± $1.11\text{x}10^{9}$ μm^3 (Figure 3A-B). Quantitative analysis of alloxan-treated rats showed a significant decrease in BCM ($p<0.001$), where uptake of ^{111}In-exendin-3 (17.27 ± 2.04 kBq) and β-cell volume ($3.13\text{x}10^{9}$ ± $7.17\text{x}10^{8}$ μm^3) dropped to 23% and 26.5%, respectively, when compared to the healthy group. Quantification of ^{111}In-exendin-3 uptake in splenic, gastric and duodenal lobes, showed inhomogeneous distribution of ^{111}In-exendin-3

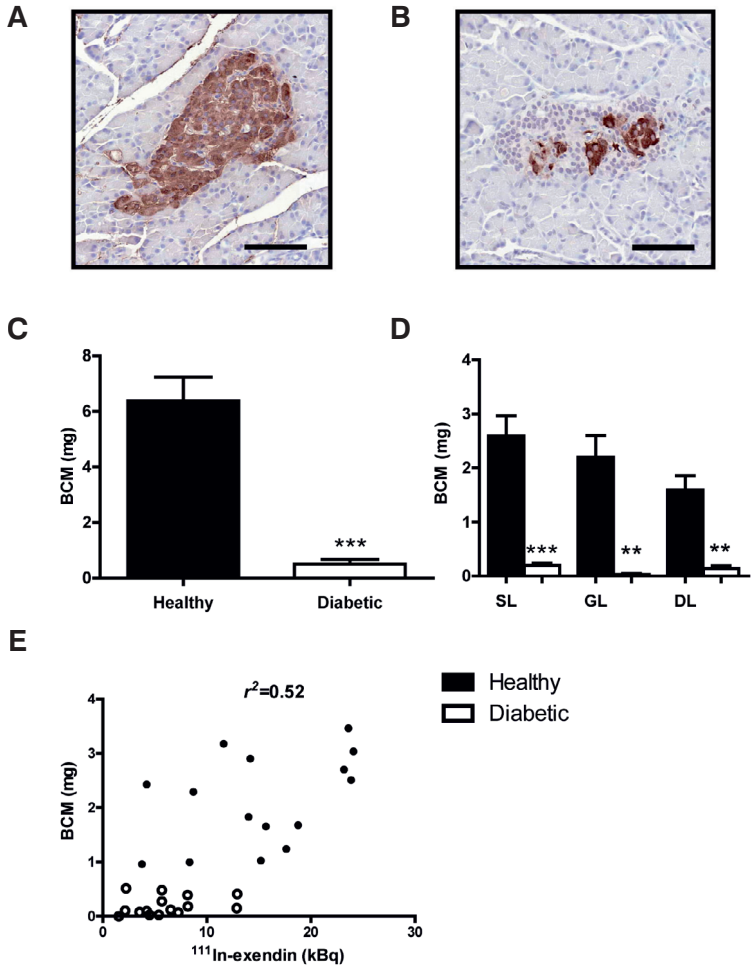

Figure 1 Histological quantitative analysis of BCM correlates with ^{111}In-exendin-3 uptake.

(***A***, ***B***) Representative images of insulin positive areas in control (A) and alloxan treated (B) rats. (***C***) Bar chart displaying BCM (mg) (n=5). (***D***) Graph displaying quantitative analysis of β-cell inter-lobular distribution (n=4-5). (***E***) BCM (mg) was plotted against ^{111}In-exendin-3 uptake (kBq, kilobecquerels) as determined by SPECT (r^2=0.52, p=8.13 x 10^{-06}). In (A-E) untreated rats are shown in black and alloxan-treated rats are shown in white. Data are shown as means ± SEM, where *p<0.05, **p<0.01 and ***p<0.001 compared with the corresponding healthy group. Scale bar represents 100 μm.

accumulation between the lobes, as the uptake was 22.06 ± 1.48, 10.58 ± 2.72 and 14.57 ± 2.55 kBq, respectively (Figure 3C). A similar distribution pattern was observed by OPT, where β-cell volume in splenic, gastric and duodenal lobes was equal to $4.90x10^9 \pm 5.81x10^8$, $3.14x10^9 \pm 6.72x10^8$ and $3.61x10^9 \pm 6.25x10^8$ μm^3, respectively (Figure 3D). Alloxan treatment resulted in decreased exendin uptake (measured by SPECT) and β-cell volumes (measured by OPT) in all lobes. The linear correlation (r^2) between exendin-3 uptake and β-cell volume per lobe was 0.77 (Figure 3E), and for total BCM 0.81 (Supplementary Figure S1 C).

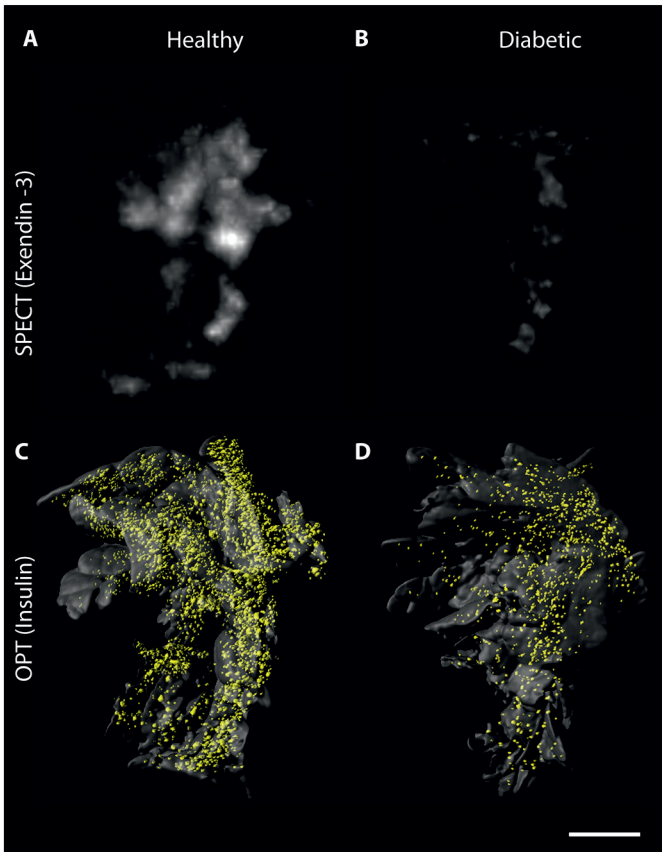

Figure 2 Multimodal imaging of pancreatic β-cells with SPECT and OPT.

(***A***, ***B***) *Ex vivo* SPECT scans of representative splenic lobes from a healthy (A) and an alloxan treated animal (B) respectively. (***C***, ***D***) OPT generated iso-surface images of the same lobes as visualized in (A, B). Alloxan-treated rats exhibit lower ^{111}In-exendin-3 uptake and β-cell volume when compared to the control group. Scale bar represents 3 mm.

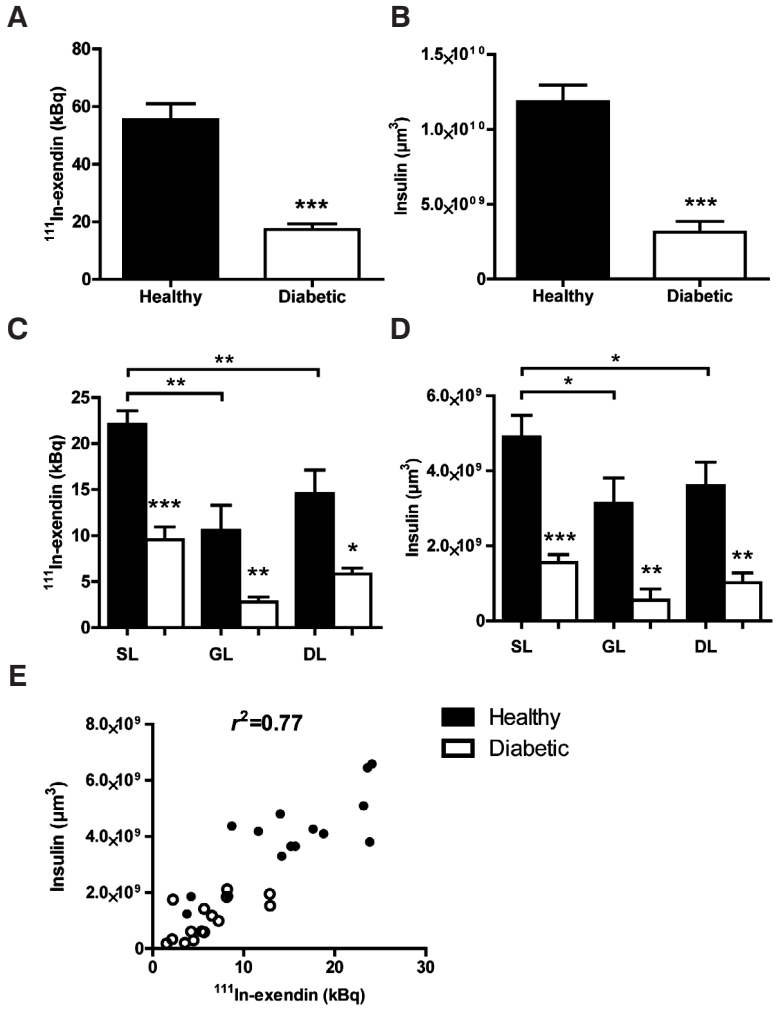

Figure 3 SPECT based radioactive quantification of ^{111}In-exendin-3 uptake correlates with OPT based quantification of insulin positive β-cell volume.

(***A***, ***B***) Quantification of absolute ^{111}In-exendin-3 uptake (kBq) by SPECT (A) and total β-cell volume (μm^3) by OPT (B) (n=5). (***C***, ***D***) Graphs illustrating the heterogeneous distribution of β-cells between the splenic (SL), gastric (GL) and duodenal lobes (DL) as determined by SPECT (C) and OPT (D) respectively (n=4-5). (***E***) Graph showing pancreatic uptake of ^{111}In-exendin-3 by separate lobes plotted against β-cell volume shows a strong correlation (r^2=0.77, p=2.07 x 10^{-10}). In (A-E) untreated rats are shown in black and alloxan-treated rats are shown in white. Data are shown as means ± SEM, where *p<0.05, **p<0.01 and ***p<0.001 compared with the corresponding healthy group.

Importantly, SPECT data was successfully compared with OPT analysis of the entire islet population of each pancreas within a time period during which only a limited number of intervallic sections per lobe could be analyzed by stereology. Furthermore, SPECT-OPT correlation (r^2=0.77) was significantly superior to SPECT-histology (r^2=0.52) ($p<0.001$). There were no significant differences between the linear regression slopes ($p=0.82$) (Supplementary Figure S2 B).

Discussion

In the present study, we examined the utility of SPECT-OPT multimodal imaging for fast and accurate validation of radionuclide-based imaging of β-cells. The successful imaging of β-cells by SPECT and OPT, respectively, demonstrated the possibility of combining the protocols of both imaging modalities. ^{111}In-exendin-3 uptake and insulin volume as measured by SPECT and OPT were in excellent linear correlation, demonstrating that the performance of β-cell radiotracers can be cross-examined by OPT. Decreased OPT signal subsequent to alloxan treatment was in line with SPECT signal, further demonstrating that the data generated using OPT are consistent with measurements obtained by SPECT.

While the resolution provided by conventional microscopy prevails over OPT, correlation of insulin staining with exendin-3 uptake by immunohistochemical analysis was significantly lower, indicating that stereological methods may be less accurate than OPT for validating SPECT-based quantification of BCM, mainly because they are prone to BCM quantification errors. Including more histological sections into the quantitative analysis for each lobe would be expected to increase the BCM quantification accuracy, but would also be more labor and time-consuming. In contrast, excellent linear correlation was achieved in a similar period of time, by combining SPECT and OPT imaging, where quantification of tracer uptake was followed by a single acquisition of the entire insulin positive cell population of intact pancreatic lobes [8], thus comparing three-dimensional data sets.

Assessment of *islet* spatial heterogeneity with histology was challenging, given the two-dimensional aspect of the method. On the other hand, inhomogeneous distribution of the islets between the pancreatic lobes was evident by SPECT and OPT. The splenic lobe harbored the largest BCM, followed by the duodenal and the gastric lobes respectively, which is in agreement with the β-cell distribution previously recorded for the murine pancreas [9]. Furthermore, the distribution of ^{111}In-exendin-3 in alloxan treated pancreata was, not only quantitatively, but also visually in agreement with OPT (figure 1). Residual β-cells in alloxan-treated rats were mainly observable in the core of the lobes, an area also showing the highest accumulation of ^{111}In-exendin-3. The excellent correspondence between SPECT and OPT spatial information endorses

the previously reported radiotracer specificity towards the β-cells [7]. Therefore, SPECT-OPT multimodal imaging allows validation of radiotracer biodistribution in the pancreas, including information with respect to β-cell spatial heterogeneity, which renders this methodology highly convenient when validating established radiotracers and evaluating the specificity and performance of novel β-cell radiotracers.

In conclusion, we report the successful multimodal imaging of pancreatic islets after coupling protocols from two independent approaches, into one that combines radionuclide and optical imaging of β-cells. Excellent correlation between ^{111}In-exendin uptake and insulin volume was obtained by SPECT-OPT, when compared to SPECT followed by histology, demonstrating that this new strategy may be more reliable in validating the actual performance of β-cell radiotracers. In addition, as compared to morphometric analysis of pancreatic sections, OPT is highly time-efficient.

References

1. *IDF Diabetes Atlas, 7 ed., Brussels Belgium: International Diabetes Federation.* 2015.
2. Meier, J.J. and R.C. Bonadonna, *Role of Reduced β-Cell Mass Versus Impaired β-Cell Function in the Pathogenesis of Type 2 Diabetes.* Diabetes Care, 2013. **36**(Supplement 2): p. S113-S119.
3. Sherry, N.A., E.B. Tsai, and K.C. Herold, *Natural History of β-Cell Function in Type 1 Diabetes.* Diabetes, 2005. **54**(suppl 2): p. S32-S39.
4. Meier, J.J., et al., *Functional Assessment of Pancreatic β-Cell Area in Humans.* Diabetes, 2009. **58**(7): p. 1595-1603.
5. Wild, D., et al., *Exendin-4–Based Radiopharmaceuticals for Glucagonlike Peptide-1 Receptor PET/CT and SPECT/CT.* Journal of Nuclear Medicine, 2010. **51**(7): p. 1059-1067.
6. Wang, Y., et al., *Synthesis and evaluation of F-18-exendin as a potential biomarker to measure pancreatic beta-cell mass.* J NUCL MED MEETING ABSTRACTS, 2010. **51**(2_MeetingAbstracts): p. 195-.
7. Brom, M., et al., *Non-invasive quantification of the beta cell mass by SPECT with 111In-labelled exendin.* Diabetologia, 2014. **57**(5): p. 950-959.
8. Alanentalo, T., et al., *Tomographic molecular imaging and 3D quantification within adult mouse organs.* Nat Meth, 2007. **4**(1): p. 31-33.
9. Hörnblad, A., A. Cheddad, and U. Ahlgren, *An improved protocol for optical projection tomography imaging reveals lobular heterogeneities in pancreatic islet and β-cell mass distribution.* Islets, 2011. **3**(4): p. 204-208.
10. Alanentalo, T., et al., *Quantification and Three-Dimensional Imaging of the Insulitis-Induced Destruction of β-Cells in Murine Type 1 Diabetes.* Diabetes, 2010. **59**(7): p. 1756-1764.
11. Skau, M., et al., *Linear Correlation Between the Total Islet Mass and the Volume-Weighted Mean Islet Volume.* Diabetes, 2001. **50**(8): p. 1763-1770.
12. Sharpe, J., et al., *Optical Projection Tomography as a Tool for 3D Microscopy and Gene Expression Studies.* Science, 2002. **296**(5567): p. 541-545.
13. Eriksson, A.U., et al., *Near Infrared Optical Projection Tomography for Assessments of β-cell Mass Distribution in Diabetes Research.* 2013(71): p. e50238.
14. Hörnblad, A., et al., *Impaired Spleen Formation Perturbs Morphogenesis of the Gastric Lobe of the Pancreas.* PLoS ONE, 2011. **6**(6): p. e21753.

Supplemental data

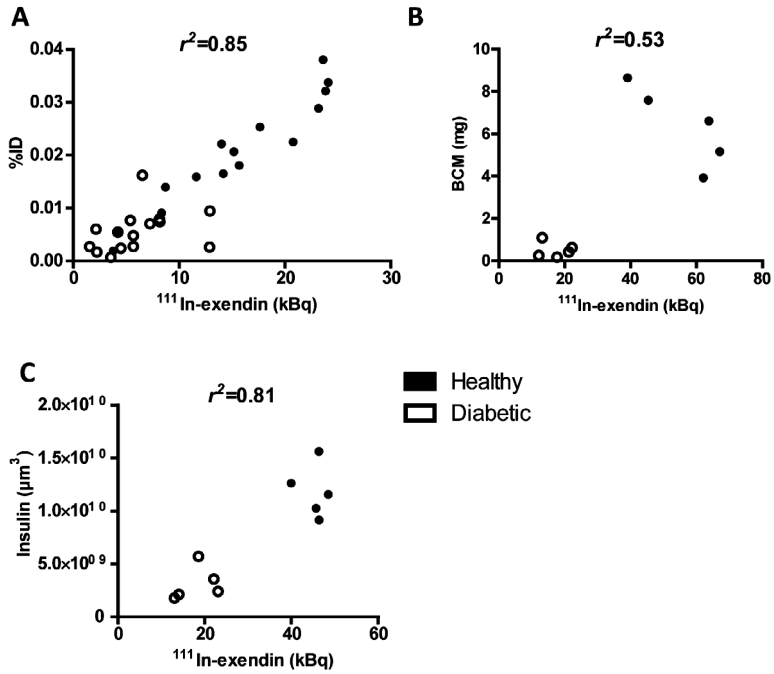

Figure S1 Linear correlations between ^{111}In-exendin-3 uptake and BCM.

(***A***) Correlation of SPECT data (kBq) with gamma-counter analysis (%ID, percentage of injected dose) of separate pancreatic lobes (r^2=0.85, p=5.55x10^{-12}) (n=15)**.** (**B, *C***) graphs showing total pancreatic uptake of ^{111}In-exendin-3 (SPECT) plotted against total BCM (histology) (r^2=0.53, p=0.017) and total pancreatic β-cell volume (OPT) (r^2=0.81, p=0.0004) respectively (n=5).

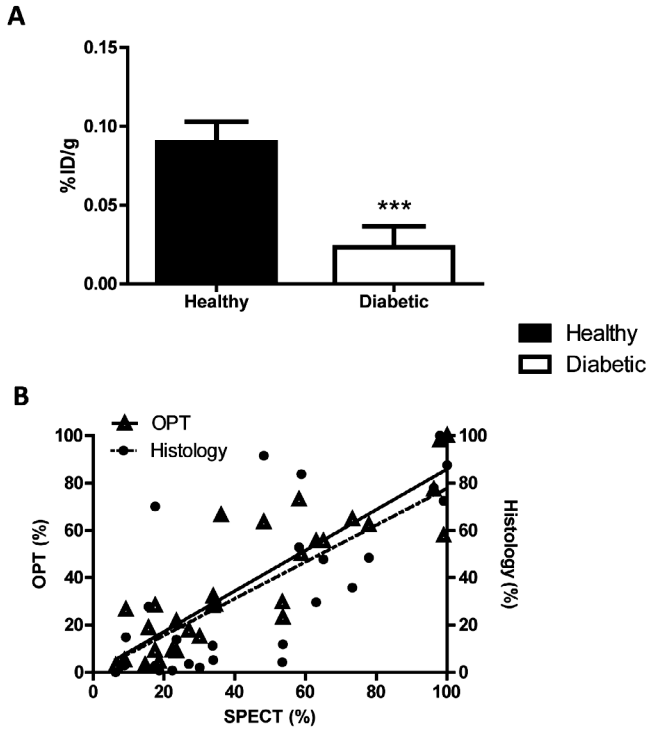

Figure S2 Alloxan treated rats display a significantly reduced uptake of ^{111}In-exendin-3.

(***A***) The Graph illustrates the pancreatic uptake of radioactivity normalized by the weight of the pancreas (%ID/g, percentage of injected dose per gram) of healthy control animals and alloxan treated animals as measured by gamma-counter. (***B***) Two-way dependent correlation coefficients comparison (SPECT-OPT r^2=0.77, SPECT-histology r^2=0.52; n=30) reveals significant differences between SPECT-OPT and SPECT-histology correlations ($p<0.001$). ANCOVA analysis reveals no significant differences between SPECT-OPT and SPECT-histology linear regression slopes ($p=0.82$). Data are expressed in relation to (%) the highest BCM value measured in a lobe by the corresponding modality.

7

Conclusion and future perspectives

1. Use of ^{111}In-exendin for effective and non-invasive quantification of BCM in transplanted islets

Transplantation of islets of Langerhans is an innovative experimental approach to reverse hyperglycemia in patients with long history of type 1 diabetes and with frequent episodes of hypoglycemia [1]. To date, the number of recipients that remain insulin independent 5 years after transplantation is as low as 15% and the current clinical tests cannot determine if graft failure originates from β-cell loss or decline in function [2]. Non-invasive imaging is therefore needed to quantify the number of living β-cells.

Quantification of pancreatic BCM by SPECT imaging with ^{111}In-exendin was previously achieved in a rat model for diabetes, as well as in healthy and diabetic subjects, and might be useful to detect β-cell loss [3]. The main objective of the studies described in this thesis was to characterize ^{111}In-exendin imaging strategy to quantify BCM which could help improving the outcome of islet transplantation.

Islet isolation disrupts the blood vessels between the islets and the surrounding tissue, which, depending on the transplantation site, would require several weeks to be completely restored. In **Chapter 3**, we demonstrated that disruption of the islet vasculature from the surrounding tissue after isolation, has great influence on the radiotracer targeting properties towards the islets, and BCM quantification using ^{111}In-exendin. Revascularization progress in the graft improves radiotracer uptake in the islets. Complete restoration of islet vasculature in the transplant allows reproducible accumulation of ^{111}In-exendin in the graft, for reproducible quantitative imaging of the islets, 4 weeks after transplantation. In **Chapter 4**, injection of ^{111}In-exendin, 4 weeks after transplantation, in recipients that received different amounts of islets allowed to quantify BCM with high accuracy and with high sensitivity. In particular, a linear correlation was observed between SPECT signal of ^{111}In-exendin uptake and the amount of β-cells that were successfully engrafted. Detection and accurate quantification of BCM was even achievable in recipients that were injected with an initial amount of 50 islets.

Stable expression of the GLP-1R is required for reliable quantification of the BCM. Under homeostatic blood glucose levels, GLP-1R expression is expected to be stable, allowing reliable quantification of the BCM. However, it was previously demonstrated that chronic exposure to hyperglycemia leads to downregulation of the GLP-1R in pancreatic β-cells [4]. This could influence radiotracer uptake by the graft, and consequently, influencing the imaging results, which leads to erroneous quantification of the actual BCM. In **Chapter 5**, we demonstrated that ^{111}In-exendin uptake in islet grafts is influenced by changes in blood glucose levels. Elevated blood glucose levels lead to decrease in tracer accumulation in the graft. Re-establishment of normal glycemic levels restored tracer uptake in the graft, indicating the direct influence of glycemia on quantification of BCM.

Determination of BCM was based on a stereological approach, where β-cell areas in graft micro-sections were extrapolated to 3D data of complete graft volumes. For accurate determination of graft volumes, it was therefore necessary to section the entire muscle tissue. In **Chapter 6**, an alternative method was suggested, in the pancreas, where BCM could be easily determined, without requiring the sectioning of a complete organ: We have used OPT as a reliable alternative to histology to validate exendin-based quantification of BCM. The method allowed visualizing the entire β-cell population of a pancreas in a single acquisition and with high accuracy when compared to histology.

2. Implications and future perspectives

Use of radiolabeled exendin for monitoring of islet grafts has an excellent clinical potential: (1) radiolabeled-exendin is clinically approved, which facilitates its clinical implementation in the context of islet graft imaging. (2) The radiotracer successfully detects islet grafts in transplantation sites that are clinically relevant (i.e. the liver) or in skeletal muscle [5, 6].

Delivery of radiotracers to transplanted islets – Tracer uptake by islet grafts depends on the speed of recovery of islet vasculature, which has significant implications on BCM quantification. Several factors could affect the delivery of radiotracers and the time-point after which intra-islet vasculature is restored: (1) Different organs inherently have different angiogenic potential. Typically, the skeletal muscle has different angiogenic potential, when compared to other known transplantation sites, such as the interior chamber of the eye and the liver [7, 8]. As a result, vascular density in the islet graft could differ between different sites, which could have a direct influence on the amount of radiotracers that accumulate in the islets. Interestingly, tracer uptake was detected as early as 3 days after transplantation, where vascular density was very low. (2) Angiogenesis might be suboptimal in recipients with long-history of diabetes, which could influence the amount of radiotracers accumulating in the graft. (3) Changes in the blood flow; We observed that diabetic islet-recipients that underwent severe and long-standing episode of hyperglycemia, and received insulin treatments prior to injection of ^{111}In-exendin, had higher tracer accumulation in the graft when compared to diabetic recipients that received no insulin treatments. Graft revascularization is completed 4 weeks after transplantation and therefore, changes in tracer uptake could potentially be explained by changes in blood flow, which is decreased during hyperglycemia. Hyperglycemia could also affect tracer uptake through other players stated below.

Quantification of BCM in islet grafts – ^{111}In-exendin allows visualization of grafts containing less than 50 islets in small animal models, indicating high sensitivity for detection of even a small beta cell mass. Exendin-SPECT imaging could therefore allow highly sensitive detection of small grafts that underwent severe β-cell loss, and in this way, might facilitate treatment assignment or adaptation in order to preserve remaining islets that could still exert a positive effect on glucose homeostasis. Such advanced sensitivity was not achieved by other β-cell markers currently under investigation, e.g. ^{123}I-IBZM [9].

Pre-labeling of islet transplants with SPIOs-MRI showed promising results for quantification of islet graft volume in humans. However, a standardized labeling protocol is needed and therefore a quantitative method is still missing. Furthermore, islet labeling does not allow to visualize the β-cells specifically, which is inconvenient when quantification of BCM is desired. Clearly, the advanced detection sensitivity and the specific quantification of β-cells by exendin-SPECT will be of great value for human applications in the future.

It was previously demonstrated that β-cell loss can be detected with ^{111}In-exendin-SPECT. Whether this strategy allows to follow-up changes in BCM over-time after multiple injections of ^{111}In-exendin must be evaluated in future studies.

Imaging the GLP-1R during diabetes – Reduced accumulation of ^{111}In-exendin in islet transplants was evident after long exposure to severe hyperglycemia. Decreased exendin-3 uptake in the graft during hyperglycemia is in line with clinical observations, where hyperglycemia contributes to impaired action of incretins on the beta cells in type 2 diabetes patients [10]. One possible explanation for reduced radiotracer uptake is downregulation of the GLP-1R [11]. Another possibility, is that exendin-3 internalization after binding to the GLP-1R is hampered by changes in the downstream signaling pathways, causing less efficient trapping of the tracer inside the beta cells [12]. Reversal of hyperglycemia with insulin injections restored tracer uptake in the graft, which could be explained by the recovery of GLP-1R expression and/or the downstream internalization pathways of the receptor. Overall, normoglycemia should be achieved prior to imaging of the GLP-1R, in order to alleviate β-cell stress and for reliable quantification of BCM.

Novel approach for validating beta cell radiotracers – We have described OPT as a reliable alternative to histology to validate exendin-based quantification of BCM. The method allowed visualizing the entire β-cell population of a pancreas in a single acquisition and with high accuracy when compared to histology. Whether OPT would be an alternative to histology for validating ^{111}In-exendin imaging of islet transplants must be addressed in future studies. Interestingly, OPT was previously used to quantify BCM of islets transplanted in the liver [13], a transplantation site that is

clinically relevant and which will take part of our future work to validate islet graft imaging with ^{111}In-exendin.

In conclusion, we characterized a method for non-invasive monitoring of transplanted islets using ^{111}In-exendin followed by SPECT imaging. Our strategy could potentially quantify graft survival, and in combination with β-cell functional tests, could provide clinicians with a comprehensive information about islet graft quality.

References

1. Scharp, D.W., et al., *Insulin Independence After Islet Transplantation Into Type I Diabetic Patient.* Diabetes, 1990. **39**(4): p. 515-518.
2. Ryan, E.A., et al., *Five-Year Follow-Up After Clinical Islet Transplantation.* Diabetes, 2005. **54**(7): p. 2060-2069.
3. Brom, M., et al., *Non-invasive quantification of the beta cell mass by SPECT with 111In-labelled exendin.* Diabetologia, 2014. **57**(5): p. 950-959.
4. Xu, G., et al., *Downregulation of GLP-1 and GIP Receptor Expression by Hyperglycemia: Possible Contribution to Impaired Incretin Effects in Diabetes.* Diabetes, 2007. **56**(6): p. 1551-1558.
5. Pattou, F., J. Kerr-Conte, and D. Wild, *GLP-1-receptor scanning for imaging of human beta cells transplanted in muscle.* N Engl J Med, 2010. **363**(13): p. 1289-90.
6. Wu, Z., et al., *In Vivo Imaging of Transplanted Islets with 64Cu-DO3A-VS-Cys40-Exendin-4 by Targeting GLP-1 Receptor.* Bioconjugate Chemistry, 2011. **22**(8): p. 1587-1594.
7. Nyqvist, D., et al., *Donor Islet Endothelial Cells in Pancreatic Islet Revascularization.* Diabetes, 2011. **60**(10): p. 2571.
8. Jones, G.L., et al., *Time Course and Quantification of Pancreatic Islet Revascularization Following Intraportal Transplantation.* Cell Transplantation, 2007. **16**(5): p. 505-516.
9. Willekens, S.M.A., et al., *SPECT of Transplanted Islets of Langerhans by Dopamine 2 Receptor Targeting in a Rat Model.* Molecular Pharmaceutics, 2016. **13**(1): p. 85-91.
10. Holst, J.J., et al., *Loss of Incretin Effect Is a Specific, Important, and Early Characteristic of Type 2 Diabetes.* Diabetes Care, 2011. **34**(Supplement 2): p. S251.
11. Rajan, S., et al., *Chronic hyperglycemia downregulates GLP-1 receptor signaling in pancreatic β-cells via protein kinase A.* Molecular Metabolism, 2015. **4**(4): p. 265-276.
12. Brom, M., et al., *Radiolabelled GLP-1 analogues for in vivo targeting of insulinomas.* Contrast media & molecular imaging, 2012. **7**(2): p. 160-166.
13. Eriksson, A.U., et al., *Near Infrared Optical Projection Tomography for Assessments of β-cell Mass Distribution in Diabetes Research.* Journal of Visualized Experiments : JoVE, 2013(71): p. 50238.

Summary

Summary

The objective of the studies in the present thesis was to characterize the GLP-1R as a potential target to visualize and determine the survival of transplanted islets *in vivo*. **Chapter 2** provides an overview of the strategies that are used in nuclear medicine to visualize and quantify BCM of islet transplants and the animal models that can be used to characterize and validate new β-cell radiotracers. Several strategies were exploited over the last decade to visualize and quantify islet survival after transplantation, which demonstrated the potential of Nuclear Medicine Imaging in monitoring islet survival with high sensitivity. Overall, these strategies required labeling of the islets with radioactive probes prior to transplantation, if not the necessity to genetically modify the β-cells in order to express the radiotracer target receptor. Our study emphasizes on *in vivo* targeting of β-cells as an approach which allow visualizing islet transplants, without having the necessity to manipulate the islets *in vitro*, prior to transplantation (e.g. labeling with contrast agents and genetic modification of the β-cells). While different transplantation sites can be used to validate β-cell radiotracers (e.g. the liver, subcutaneous spaces, kidneys), we suggest the muscle as a convenient transplantation site that confines the islets in a small area, allowing easy visualization and histological quantification of BCM and the subsequent validation of radiotracers in animal models.

Isolation of islets disrupts their vasculature and requires several weeks to restore completely after transplantation. As demonstrated in **Chapter 3,** exendin uptake was evident in freshly isolated islets, as well as in the first days after transplantation, suggesting the presence of GLP-1R in the first days after transplantation. However, delivery of ^{111}In-exendin to the islets was optimal and reproducible 4 weeks after transplantation, when islet vasculature was completely restored. Consequently, quantification of BCM was possible in 4-week old islet grafts, evidenced by the linear correlation between tracer accumulation in the graft and insulin volume (**Chapter 4**). After determination of the optimal time-point for accurate quantification of BCM in islet transplants, in **Chapter 5** we examined the effect of hyperglycemia on the accumulation of ^{111}In-exendin in the β-cells. Our data indicated hyperglycemia decreases tracer accumulation in the islets. Most importantly, re-establishing normoglycemia subsequent to a period of hyperglycemia allowed to restore the uptake of ^{111}In-exendin by the islets, suggesting that normalized blood glucose levels should be achieved prior to SPECT imaging, in order to monitor BCM in a reliable manner.

In **Chapter 6**, We have determined OPT as an accurate and easy method to validate exendin-based quantification of BCM in animal models. Excellent linear correlation between ^{111}In-exendin uptake and insulin volume was achieved by SPECT-OPT, when compared to SPECT followed by histology, demonstrating that this new method may be more accurate in evaluating the performance of β-cell radiotracers during future studies.

Samenvatting

Samenvatting

In dit proefschrift wordt het onderzoek beschreven om de eilandjes van Langerhans *in vivo* zichtbaar te maken door middel van targeting van de glucagon-like peptide-1 receptor. Op deze manier wordt het mogelijk om de hoeveelheid overlevende eilandjes van Langerhans na transplantatie, een experimentele behandeling voor diabetes type 1, te bepalen. In **Hoofdstuk 2** wordt een overzicht gegeven van het onderzoek om getransplanteerde eilandjes van Langerhans zichtbaar te maken met behulp van radionuclide beeldvorming. Bovendien wordt een overzicht gegevens van de diermodellen die beschikbaar zijn om nieuwe radiotracers voor targeting van beta cellen (in de eilandjes van Langerhans) te valideren. Het laatste decennium zijn er verschillende technieken gebruikt om eilandjes van Langerhans te visualiseren. Een voorbeeld van deze methodes is het preïncuberen van de eilandjes met de radiotracer voordat de eilandjes getransplanteerd worden. Een ander voorbeeld is het genetisch manipuleren van de eilandjes van Langerhans, zodat ze een eiwit tot expressie brengen die gebruikt kan worden voor targeting met een bekende radiotracer. Het nadeel van deze technieken is dat manipulatie van de eilandjes van Langerhans voor de transplantatie noodzakelijk is. Het onderzoek beschreven in dit proefschrift richt zich op een methode waarbij gebruikt wordt gemaakt van targeting van een receptor die al van nature op de beta cellen tot expressie komt. Deze methode maakt directe targeting van de beta cellen mogelijk, zonder dat de eilandjes vooraf gemanipuleerd hoeven te worden.

Verschillende locaties voor de transplantatie van eilandjes van Langerhans in diermodellen zijn beschreven, bijvoorbeeld in de lever, nier of onderhuids. Voor onze studies hebben we gebruik gemaakt van transplantatie in de spier, waarbij de eilandjes van Langerhans dicht bij elkaar in een klein gebied zitten. Dit maakt het makkelijk om de hoeveelheid eilandjes met behulp van histologische technieken te bepalen. Bovendien is het met dit model eenvoudig om het transplantaat zichtbaar te maken met radionuclide beeldvorming.

Na de isolatie procedure van de eilandjes van Langerhans uit de alvleesklier en de transplantatie procedure is het bloedvat netwerk van de eilandjes verloren gegaan. Voor een goede overleving en functie van de getransplanteerde eilandjes is het noodzakelijk dat dit bloedvat netwerk weer hersteld wordt. Voorgaande studies hebben aangetoond dat het 4 tot 6 weken duurt voor het bloedvat netwerk weer volledig hersteld is, afhankelijk van de locatie van transplantatie. De afwezigheid van bloedvaten kan invloed hebben op de opname van de radiotracer die gebruikt wordt in onze studies: exendin. In **Hoofstuk 3** hebben we onderzocht wat het optimale tijdpunt is voor het afbeelden van getransplanteerde eilandjes. Direct na isolatie en de eerste dagen na transplantatie was er opname van radiogelabeld exendin te zien, wat suggereert dat de GLP-1R aanwezig is. De opname van radiogelabeld exendin in

het transplantaat nam met de tijd toe en was stabiel na vier weken na transplantatie. De stabilisering van de opname was in lijn met de herstellen van het bloedvat netwerk, wat ook na 4 weken niet meer toe nam. In Hoofdstuk 4 is aangetoond dat de hoeveelheid eilandjes van Langerhans in het transplantaat een lineaire correlatie heeft met de hoeveelheid opname van radiogelabeld exendin. Deze resultaten tonen aan dat het mogelijk is om de hoeveelheid eilandjes van Langerhans te bepalen met behulp van een exendin scan.

Nadat het optimale tijdpunt voor een exendin scan en de correlatie tussen de hoeveelheid eilandjes en opname van radiolgelabeld exendin bepaald was hebben we het effect van hoge bloedglucose waarden op de opname van radiogelabeld exendin in de eilandjes van Langerhans bepaald in **Hoofdstuk 5**. We hebben aangetoond dat muizen (getransplanteerd met eilandjes van Langerhans) die hoge bloedglucose waarden hadden, minder opname van radiogelabeld exendin in de eilandjes van Langerhans hadden. Dit effect was omkeerbaar: nadat de muizen weer normale bloedglucose waarden hadden was de opname van radiogelabeld exendin in de eilandjes vergelijkbaar met de opname in gezonde muizen die gedurende het gehele experiment normale bloedglucose waarden hadden.

In **Hoofdstuk 6** hebben we een nieuwe methode om de hoeveelheid beta cellen te meten in alvleesklier weefsel vergeleken met de traditionele histologische methode. De 3-dimensionale techniek Optical Projection Tomography (OPT) maakt het mogelijk om de beta cellen in de gehele alvleesklier van een zichtbaar te maken en te kwantificeren. Met de traditionele histologische methode is het alleen mogelijk om op 2-dimensionale doorsnedes van het weefsel de hoeveelheid te bepalen. We hebben aangetoond dat het meten van de hoeveelheid beta cellen met OPT een snelle, betrouwbare en accurate methode is voor het meten van de beta cellen en dat deze methode in de toekomst gebruikt kan worden voor het karakteriseren van beta cel tracers.

List of publications

List of publications

1. **Wael A. Eter**, Saba Parween, Lieke Joosten, Cathelijne Frielink, Maria Eriksson, Maarten Brom, Ulf Ahlgren, Martin Gotthardt. *SPECT-OPT multimodal imaging enables accurate evaluation of radiotracers for β-cell mass assessments. Scientific Reports* **6**, 24576, doi: 10.1038/srep24576 (2016).

2. **Wael A. Eter**, Desiré Bos, Cathelijne Frielink, Otto C. Boerman, Maarten Brom, Martin Gottardt. *Graft revascularization is essential for non-invasive monitoring of transplanted islets with radiolabeled exendin*. *Scientific Reports* **5**, 15521, doi:10.1038/srep15521 (2015).

3. **Wael A. Eter**, Inge van der Kroon, Karolina Andralojc, Mijke Buitinga, Stefanie M.A. Willekens, Cathelijne Frielink, Desiree Bos, Lieke Joosten, Otto C Boerman, Maarten Brom, Martin Gotthardt. *Non-invasive in vivo determination of viable islet graft volume by radiolabeled exendin-3. Scientific Reports* **5**, 15521, doi:10.1038/s41598-017-07815 (2017).

4. Maarten Brom, **Wael A. Eter**, Inge van der Kroon, Stefanie M.A. Willekens, Annemarie Eek, Marti Boss, Mijke Buitinga, Martin Gotthardt. *Beta-cell imaging as part of "Imaging on Metabolic Diseases".* In: In: Kiessling F., Pichler B., Hauff P. (eds) Small Animal Imaging. Springer, Cham. doi: https://doi.org/10.1007/978-3-319-42202-2_24

5. **Wael A. Eter**, Mijke Buitinga, Cathelijne Frielink, Maarten Brom, Martin Gotthardt. *Effect of hyperglycemia on quantification of β-cell mass with radiolabeled exendin*. In preparation.

6. Filippo C. Michelotti, Gregory Bowden, **Wael A. Eter**, Volker Nischwtiz, Maarten Brom, Martin Gotthardt, Andreas Maurer, Andreas M. Schmid, Bernd J. Pichler. *Validation of a PET – ME-MRI method for in vivo evaluation of transplanted islets of ß-cells.* In preparation.

Acknowledgements

Acknowledgements

This present PhD thesis is the result of 4 years of hard work, which could not have been accomplished without the help and support of many colleagues.

My PhD thesis was part of an innovative research network, BetaTrain, that assembled top European research groups in the field of beta cell imaging, coordinated by **Prof. Dr. Martin Gotthardt**.

Martin, I would like to express my gratitude for your continuous support during my entire thesis. Your guidance and advices have truly influenced my way of working and reasoning as a Biomedical Scientist. Most importantly, you have believed in me during my hard moments at work, and you did your best to set my thesis back on track whenever needed. Joining your research group was one of the best experience I've had throughout my early career.

Dr. Brom, dear Maarten, I thank you for your daily support, advices and guidance. You have been a great supervisor and a great friend. Working with you gave me the true sense of confidence, and was a key success for my thesis.

Prof. Boerman, dear Otto, you were closely involved in my research projects and I truly appreciate your support, your great advices throughout my entire thesis. I am proud to have been part of your research group.

Cathelijne, **Lieke** and **Desiree**, your help was a key for my successful PhD thesis. The transfer of my thesis from Geneva to Nijmegen was a tough event for me, but you have made sure that I integrate fast in the group and produce all the results we needed within a short period of time to answer challenging research questions. Working with you was always fun and motivating. **Bianca**, **Kitty**, and **Iris**, thank you for your tremendous help during my experiments since the first day of my thesis.

Selen, Annemarie, Willem, **Charlotte**, **Tessa**, **Stefanie**, **Marlène** and **Tom**, I am happy I have met you and to have worked in the same office with most of yo. Thank you for supporting me throughout my thesis and for all the fun we have had in the last 4 years. It was great working with you as your presence was always so refreshing to me inside and outside work.

Mijke, special thanks to you for the fun times and the great work we've accomplished together – I wish we had the chance to collaborate for a longer period of time as convinced as I am to have found the perfect research partner to work with.

I thank my fellow lab mates, **Sandra**, **Marti**, **Mark**, **Daphne**, **Danny**, **Gerben**, **Janneke,** among many others, for being such great colleagues and for the fun time at the department.